CELL ADHESION: CHARACTERIZATION OF ADHESIVE FORCES AND EFFECT OF TOPOGRAPHY

By

LEE CHENG ZHAO

A THESIS PRESENTED TO THE GRADUATE SCHOOL
OF THE UNIVERSITY OF FLORIDA IN PARTIAL FULFILLMENT
OF THE REQUIREMENTS FOR THE DEGREE OF
MASTER OF SCIENCE

UNIVERSITY OF FLORIDA

2000

ACKNOWLEDGMENTS

This thesis was created with the assistance of a great number of great people. I will try to acknowledge them all. First, my parents, Dr. Alex Zhao and Ms. Wei Zhu gave me love, encouragement, and criticism. They are the best parents any child could have. My grandparents were extraordinary role models. As a child, I had to look no further for examples of integrity, achievement, and devotion to duty than my grandparents. I have only fond memories of my youth, my uncles, aunts, and cousins were steady companions during my childhood in China. I look forward to seeing them again soon.

Dr. Anthony Brennan, my advisor has been integral to this thesis, and to my success as a person. I thank him for four years of mentoring and encouragement. Above all, he believed in me. No goal was too high to be achievable. Without him, none of this would have been possible. The other members of my supervisory committee have also been of great assistance. I especially appreciate their understanding of the rushed timing of this Master's thesis and defense. Besides helping me with my thesis, Dr. Christopher Batich influenced my interests in polymers and biomaterials considerably through his classes. I would like to thank Dr. Tran-Son-Tay for taking the time to review and critique my thesis. I greatly appreciate Dr. Andrew Rapoff for agreeing to be a substitute member of my committee at the last moment.

The students in the Brennan group, and of the Materials Science and Engineering Department as whole have made working here enjoyable. They have also been marvelous friends. In 1996 and 1997, Dr. Tom Miller showed amazing patience while skillfully teaching a clumsy and naive 17-year old undergrad how to work with organic reactions. Ms. Jennifer Russo was a wonderful collaborator and friend during my undergraduate research in 1997 and 1998. During my internship at Exxon Chemical in Baton Rouge, LA, Dr. Michael Zamora was a terrific mentor, who helped me gain a sense of how engineering in industry was conducted.

Adam Feinberg, Wade Wilkerson, and Chuck Seegert helped me with the cell adhesion portion of the thesis. Chuck created the silicon wafers and the polystyrene templates on which silicone substrates were to be cast. Chuck also kindly allowed me access to his comprehensive library of biomedical textbooks. Wade took the tedious job of manufacturing the silicone substrates used in chapter 4 of this thesis. He also performed the similarly tedious work of treating samples with radiofrequency glow discharge plasma. Adam graciously took the scanning electron micrographs (Fig 2-4, 3-2, 4-3, 4-5, and 4-6) shown in this thesis, and built a database of the different pictures. Adam, Wade, and Chuck were constant sources of advice and assistance in the cell adhesion work. I could not have accomplished this work without their help.

Many others have helped with the thesis by being great coworkers. Jeremy Mehlem deserves commendation for his charm and his tenacity—he has been in the Brennan group for over four years. I am eternally indebted to Jeanne Macdonald for her help with the formatting of this thesis, and for her friendship. I can thank Jamie Rhodes for introducing me to some of the extracurricular aspects of college. Mark Schwarz,

Jesse Arnold, John Fultz, Luxsamee Plangsangmas, Sohyun Park, Nikhil Kothurkar, Clay Bohn, and Art Gavrin have all made my times here very memorable.

Brenden Hauser is the most reliable and dedicated undergraduate I have ever worked with. He was of tremendous assistance in the work detailed in Chapters 2 and 3. He helped me perform many of the grafting reactions. He also had the patience and manual dexterity to place microspheres onto AFM tips, and to perform AFM force measurements. I am truly indebted to him for all his help.

Members of Dr. Eugene Goldberg's group also gave me much help with my thesis. Bob Hadba showed me many of the details regarding reacting proteins onto different substrates. Kaustubh Rau, Laurie Jenkins, and Mike Grumski performed some of the x-ray photoelectron spectroscopy reported in my thesis. Paul Martin and Chris Widenhouse gave me advice on sample preparation for scanning electron microscopy.

Several employees of the Major Analytical Instrumentation Center were of great help. Jacques Cuneo taught me how to use the atomic force microscope in 1997, and has been a good source of advice and insight ever since. Amelia Dempere provided me with AFM tips, and Wayne Acree was responsible for coating the SEM samples with gold and palladium.

Much of the research would have come to naught without the dedicated efforts of the secretaries. Jackie Hulsey, while in Materials from 1996 to 1998, and in Biomedical Engineering until 1999, was a great help. Her bright outlook and remarkable skills made every job easier. Shelly Burleson has been an excellent replacement for Jackie. Her sense of humor makes the office interesting.

Shadowing Dr. Keith Ozaki helped me realize that I wanted to go into medicine (and probably academic surgery) as a career. He has also been extremely generous with his time in advising, and in allowing me to work in his laboratory. I could not have found a better role model for my future career in medicine. Zaher Abouhamze and John Rectenwald in Dr. Ozaki's research group gave me assistance countless times. I thank them for being two of the nicest people I have ever worked with, and I only hope that I get to work with people like them in the future. Nina Klingman was extremely accommodating, even after my numerous errors that jeopardized the integrity of her lab. I thank her for giving me a second (and third and fourth…) chance. Bert Herrara from Dr. Edward Block's group provided the porcine vascular endothelial cells used in this study. I thank him for being very accessible and friendly.

I would also like to thank my roommates (and good friends), Chris Williams and Andy Sinclair, for putting up with my complaints, rants, and general nastiness for the past two years. I wish that I could be as nice as they are. I also appreciate my friends Katie Thomas, Julee Shamhart, Mandy Ewing, and Conor Hardeman for listening to me and battling overwhelming ennui.

During my time both as an undergraduate in Materials and as a graduate student, Martha McDonald helped me plan out my course schedule, and my life. Dr. Richard Connell first recommended me to work for Dr. Brennan. For that, and for his advice, I am deeply grateful. Mrs. Diana Brantley deserves thanks for putting me in touch with Dr. Abbaschian, who helped me greatly during the writing of the thesis.

TABLE OF CONTENTS

Page

Abstract of Thesis Presented to the Graduate School
of the University of Florida in Partial Fulfillment of the
Requirements for the Degree of Master of Science

CELL ADHESION: CHARACTERIZATION OF ADHESIVE FORCES AND EFFECT OF TOPOGRAPHY

By

Lee Cheng Zhao

August 2000

Chairman: Anthony Brennan
Major Department: Biomedical Engineering

Two aspects of cell adhesion were studied. First, the forces of interaction in the biotin/avidin and the selectin/sialyl Lewis X (SLe^X) systems were measured by bonding microspheres to cantilevers of the atomic force microscope (AFM). The effect of surface topography on cell adhesion was also studied.

Avidin/Biotin

Biotin covalently linked to poly(ethylene glycol) was grafted onto silica microspheres (r = 5mm) using 3-aminopropyltriethoxysilane (APS). Avidin was grafted onto glass slides with glutaraldehyde (Glut) and APS. Slides with only Glut were used as the control. The microspheres were bonded to AFM tips, and ten measurements of the force of interaction were taken. The Derjaguin approximation between spheres and flat plates was used to normalize force values. Free biotin at 0.5, 1, and 2 wt% was added.

An attractive force of 0.96 ± 0.15 nN/μm (mean ± SD) at a distance of 116.5 ± 26.9 nm was observed between avidin and biotin. The addition of free biotin into solution had no effect on the force.

Select/SLe^X

SLe^X covalently linked to bovine serum albumin (BSA) was grafted onto silica microspheres (r = 5mm) with Glut and APS. Microspheres with BSA grafted directly onto the surface served as the control for nonspecific interactions. Porcine vascular endothelial cells (ECs) were grown using cell culture techniques on polydimethylsiloxane (PDMS) elastomer substrates. Ten independent force measurements were made on test samples and controls as they were brought into contact with selectin expressing ECs.

There was a short-range nonspecific interaction between the microsphere and the cell surface, and a long-range specific interaction between SLe^X and the selectins. The short-range attractive interaction between SLe^X and ECs was 0.212 ± 0.040 mN/μm at 14.2 ± 3.1 nm, while that between BSA and ECs was 0.261 ± 0.062 mN/μm at 16.2 ± 2.9 nm. Between SLeX and ECs, a second interaction of 230.4 ± 40.4 pN was measured at 106.7 ± 26.0 nm. This force appeared to involve uncoiling of the selectin and rupture of the receptor-ligand bond.

Topography

ECs were grown on textured PDMS substrates with 5 μm deep and 5, 10, and 20 μm wide grooves. The ECs were investigated with optical, scanning electron, and scanning laser confocal microscopes.

The ECs proliferated on PDMS substrates coated with fibronectin or treated with radiofrequency plasma, but not on plain PDMS. The ECs also deformed the PDMS substrate, and appear to bridge the grooves between ridges.

CHAPTER 1

INTRODUCTION

Cell Adhesion in Biology

Cellular adhesion molecules are critical to the function of life. The coordination of dynamic systems of cellular adhesion affect processes such as blood vessel formation, immunological response, wound healing, blood clotting, embryonic development, and tissue organization in general. Cell adhesion creates many unexpected phenomena. For example, when embryonic cells are dissociated, the cells will reassemble into tissue resembling the original *in vitro*. Altered adhesion properties are also a characteristic of cancer cells. Thus, the applications for an improved understanding of cell adhesion are numerous. The specificity of cell adhesion comes from combinatorial expression and interaction among a large number of adhesion receptors. Adhesion receptors also act as signaling molecules by connecting to the cytoskeleton. The signaling pathways allow adhesion receptors to influence cell survival and gene expression. Most cells have anchorage dependence, meaning that they will not proliferate or survive unless they are adhering to a substrate. Signal transduction has typically fallen under the jurisdiction of receptors for growth factors. Only in the past decade have cell adhesion receptors become associated with signaling. Thus, one must consider receptors for growth factors and adhesion receptors as parts of an integrated system.

The coming fruition of the Human Genome Project and privately funded efforts at sequencing the human genome, such as the much publicized Celera Genomics effort (Rockville, Md) will reveal many trends in the cell adhesion system. Recently, the genome for the fruitfly *Drosophila melanogaster*.[1] and in 1998, the genome for the nematode *Caenorhabditis elegans* was sequenced.[2] From the information contained in these genomes, one can make several conclusions. First, in both *D. melanogaster* and *C. elegans* there are a large number of extracellular matrix proteins (ECM), much more than in the eukaryote *Saccharomyces cerevisiae* (yeast). ECM proteins appear crucial for multicellular life. Integrins, the primary receptors for ECM proteins are fewer, with seven types in the fly and three in the worm. There are at least 18 integrins in vertebrates. Cadherins, another adhesion receptor has a similar increase in complexity. There are over 70 cadherin genes in humans, while the fly has only 3, and the worm 15. The combinatorial action of the large number of adhesion molecules allows spatiotemporal regulation, and thus, the specificity observed in cell adhesion.

The complexity and ubiquity of the cell adhesion system make a quantitative study extremely important. A fundamental, theoretical understanding of cellular behavior has not been completely formulated. Since the applications of cell adhesion are so varied, I concentrated on one aspect, leukocyte adhesion to the blood vessel endothelium. In particular, I focused on the forces between specific receptors and ligands. Before any discussion of receptor-ligand interactions, a review of how cell adhesion affects the blood vessel is required.

Cell adhesion is important for the immune response in the vasculature, and by association, the creation of vascular grafts in biomaterials. First, a discussion of blood

vessels: the vascular wall is composed of three layers: the intima, the media, and the adventitia.[3] The intima is the innermost layer of the wall, and thus, is in direct contact with blood. This layer is composed of a monolayer of endothelial cells. The media is made of smooth muscle cells bounded by elastic laminae. The smooth muscle cells are embedded in a matrix of collagen, proteoglycan, and elastin. This layer is prominent in large arteries such as the aorta, and becomes thinner and less distinct as the vessel diameter decreases. The outer most layer is the adventitia, which is formed of loose connective tissue, fibroblasts, small nerve fibers, and capillaries. Obviously, cell adhesion holds all three layers together, but how cells in the blood interact with the vessel is the focus of my study.

In both the vasculature and most other tissue, the entities that mediate cell adhesion fall into three classes: adhesion receptors, extracellular matrix (ECM) molecules, and the intracellular adhesion plaque proteins. Cell adhesion receptors, such as integrins, selectins, cadherins, and members of the immunoglobulin-cell adhesion molecule (Ig-CAMs) superfamily, determine the specificity of cell-cell or cell-ECM interaction. They are transmembrane molecules that bind to ECM molecules or counter-receptors on other cells. The ECM molecules, like fibronectin and collagen, are typically fibrous proteins that create a complex network that interacts simultaneously with several cell receptors. Intracellular adhesion plaque proteins form linkages between adhesion receptors and the cytoskeleton. These linkages allow the cell to respond to changes in adhesion properties. Some examples are α and β catenins that bind with cadherins. The study of all of these adhesion molecules may be enhanced by quantitative measurements of the force of interaction between them.

The entities that dictate cell adhesion in the endothelium are mainly cell adhesion receptors. Selectins and integrins are used in combination in the inflammatory response to deliver leukocytes to the site of injury. Upon activation by the injury, endothelial cells express P- and E-selectins that weakly bind leukocytes in a process known as "rolling." Then, integrins are used to strongly attach leukocytes to the blood vessel wall. Selectins are adhesion receptors that recognize carbohydrate ligands. Three types of selectins have been identified: L, P, and E.[4] L-selectins, the first to be discovered, is expressed by leukocytes. This form of selectin participates in the adherence of leukocytes to peripheral lymph nodes, and the recruitment of neutrophils and monocytes to inflammatory sites. P-selectins was discovered by investigators interested in platelet activation,[5] and is rapidly distributed to the surface of platelets upon activation by thrombin and other mediators. E-selectins are found on the endothelium, and support the adhesion of eosinophils, neutrophils, and monocytes.

There are many applications to an improved understanding of the leukocyte adhesion process, since the adhesion molecules are involved in inflammation, wound healing, and cancer metastasis. For instance, the integrin ligand, arginine-glycine-aspartic acid (RGD) has become the basis of efforts to develop treatments.[6] Telios Pharmaceuticals of San Diego created a wound healing gel-bearing RGD to improve cell adhesion. Anti-clotting drugs are another application—Centocor Inc. of Malvern, PA markets ReoPro® (abciximab), a drug that targets the glycoprotein IIb/IIIa receptor on the surface of platelets. Another avenue of investigation is to treat inflammation by blocking selectins. Cancer cells display adhesion molecules that are much different from the complement found on normal cells. For example, it has been shown that CD44, an

adhesion molecule found on leukocytes also occurs on the surface of pancreatic tumor cells.[7]

Besides all the pharmaceutical implications, one additional clinical application for the improved understanding of cell adhesion in the vasculature is the design of synthetic vascular grafts. Prosthetic vascular grafts are used for the replacement of aneurysms, as a site for dialysis, and to revascularize tissue when veins are unavailable. Such grafts, especially smaller models (diameter < 4mm), are subject to failure from two modes: thrombogenicity and anastomotic pseudointimal hyperplasia. In the former, an inflammatory response to the foreign biomaterial (typically polyethylene terephthalate or polytetrafluoroethylene) causes thrombosis and leads to occlusion of the vessel. According to Greisler, occlusions due to thrombogenicity typically occur within six months.[8] After six months, failure of small diameter grafts is often associated with anastomotic pseudointimal hyperplasia. Both of these failure modalities are due to a mismatch in the chemical and mechanical properties between the graft and the natural blood vessel. To prevent these graft failures, biomedical engineers attempted to seed endothelial cells onto the surface of the grafts.[9, 10] The goal of endothelial cell seeding is mimicry of the vascular wall. To improve the efficacy of cell seeding, investigators have coated the graft with pyrolytic carbon.[11, 12] Other methods to avert failure include the use of heparin[13] to stop thrombosis, the binding of other antithrombic agents,[14] and the covalent linkage of peptides onto the graft surface[15, 16] to reduce platelet adhesion. The complexity of the vascular environment has hindered the development of a completely successful replacement for the human blood vessel despite some 40 years of research. A

more complete theoretical understanding of cell adhesion phenomena would help the search for a solution.

Quantitative Models of Cell Adhesion

Cell adhesion does not just depend on the receptors-ligand interactions. The behavior of the cell in flow also affects the adhesion characteristics.[17, 18] Cellular biology has provided a wealth of qualitative information regarding cell adhesion, but a rigorous quantitative model is lacking. George Bell formulated the seminal theory[19] in 1978, but his model has not been comprehensively tested. Bell's theory may be understood by considering an antibody-bearing cell and an antigen-bearing cell. There is specific density of antibodies or antigens on the cell surface. If the forward and reverse rate constants for the bond formation in solution are known, then the forces between the cells may be calculated. According to Bell, two nonspecific electrical forces create an equilibrium separation between cells. Generally, cells are negatively charged. Thus, there is a repulsive electrostatic force. There is also an attractive force between cells due to van der Waals interactions. The two forces operate at different distances, thereby creating an energy minimum at the equilibrium separation distance. Bell's calculations show the separation between lipid bilayers to be approximately 10 nm. This separation distance is what allows specific bond formation to occur. Once the cells are in proximity, receptors and ligands may diffuse to adjacent sites on the cell membrane and bind. Specific adhesion between cells depends on the reaction rates of the exact receptor-ligand system. Although the force between one receptor-ligand pair is weak, the collective whole of such interactions on the cell surface creates a strong adhesive force.

Since Bell's work, many other theories about cell adhesion have been formulated. Ward, Dembo, and Hammer studied the effects of ligand density on cell detachment.[20] During cell attachment, it is known that receptors cluster onto the cell-substrate interface, thus increasing both the ligand density and the adhesive strength. Ward *et al* assumed a one-dimensional tape peeling model[20] with two regions, a microscopic binding region and a macroscopic nonbinding region. At the edge of the nonbinding region, there is a tension T_{mac} applied at angle θ_{mac} with the substrate. Within the binding region, one assumes immobile receptors. A critical tension for cell detachment T_{crit} may be solved based on several parameters.

$$T_{crit} = \frac{N_1 k_b \Theta}{1 - \cos\theta_{mac}} \ln\left(1 + \frac{R_t K_{eq}}{A_{cell}}\right)$$

The critical tension is proportional to the ligand density N_1, and the thermal energy $k_b\Theta$, and exhibits a weak dependence on receptor number, R_t, and receptor-ligand affinity K_{eq}. The cell area is A_{cell}. Hammer *et al* also investigated the effect of flow on cell adhesion.[21] A simulation of leukocyte rolling on endothelium was performed by idealizing the cell as a hard sphere with adhesive springs and microvilli on the surface. Based on the flow velocity, a spectrum of adhesive states may be modeled, from transient adhesion, such as the leukocyte rolling in this study, to irreversible attachment.

The models of cell adhesion attempt to deal with many terms—ligand density, flow conditions, etc., I limited the scope of my work to measurements of the forces between individual receptor-ligand bonds, essentially, the receptor-ligand affinity. Analysis of the receptor-ligand interaction from a polymer physics perspective may be a

useful method toward understanding. The terms and methodologies from polymer physics may shed new light on the topic typically investigated by biologists and biochemists. Thus, a review of recent work in measuring the forces of adhesion between polymers, particularly hydrophilic polymers, is necessary.

Techniques for Force Measurements in Polymers

Before any discussion of the forces in polymer interaction, one must first discuss the techniques used to measure these forces, as the limitations of these methods have a significant impact on what can be measured. The literature contains two types of studies regarding the interaction forces between surfaces: theoretical and experimental. The experimental studies have been performed primarily through two methods: the surface force apparatus (SFA), and force measurements with the atomic force microscope (AFM). Israelachvili pioneered characterization of forces using the surface force apparatus (SFA) in 1978.[22] The surface force apparatus consists of two crossed cylinders of an atomically smooth substrate, held closely together with fluid in between. The substrate is maneuvered with a micrometer and a piezoelectric. The separation between the substrates is measured with a method known as multiple beam interference fringes. White light is introduced perpendicular to the surfaces, and from the wavelengths of the standing waves produced, the separation can be measured to within 0.2 nm. The force between the substrates is measured using a spring. Studies with the SFA have focused on silica, mica, and alumina, because of the limitation that the substrate must be atomically smooth.

Atomic Force Microscopy (AFM) is a powerful tool for imaging the morphology of materials, and for measuring the interaction forces between two surfaces. The predecessor of the AFM, the scanning tunneling microscope was invented in 1981 by Gerd Binnig and Heinrich Rohrer,[23] the instrument was quickly adapted for use as an atomic force microscope (AFM).[24] For the invention of the STM, Binnig and Rohrer won the Nobel prize in physics in 1986. The AFM has been used to measure the topography of a surface,[25, 26] the viscoelastic phase change, and the intersurface forces.

The method of using the AFM to measure intersurface forces requires the researcher to physically attach a colloid onto the cantilever. The deflection of the cantilever would be measured as the colloid is brought in contact with a flat surface. One of the researchers who pioneered investigating forces using the atomic force microscope was Pashley.[22, 27-30] He attached particles onto AFM tips, and measured the interaction forces between the two surfaces. Pashley has investigated the forces between silicon and polypropylene in aqueous solution.[30] In this study, glass spheres of 6 to 7 μm diameter were interacted with flat polypropylene surfaces in varying concentrations of NaCl in water. Since then, this colloid probe technique has been extended to measuring the forces in polymers,[31, 32] titania,[33] and gold.[34]

Recently, the AFM has been adapted for use in biology. Sagvolden, *et al.* measured the adhesion forces of cervical carcinoma,[35] and Holland, Siedlecki, and Marchant mapped the topography of platelets.[36] Within the past decade, AFM has been used to measure individual ligand-receptor debonding forces for the avidin-biotin system.[37-39] The AFM has also been adapted to recognize specific antibodies, and thus, discriminate between different molecules.[40]

Review of Polymer Interactions

The high selectivity of biological interactions may be attributed to the combination of hydrogen bonding, van der Waals, steric, hydrophobic, and electrostatic forces. In the force measurements, on must account for all these interactions. Thus, a brief review of how previous researchers have separated these forces using using both the SFA and the AFM is necessary.

There are several researchers investigating forces using the SFA, including Israelachvili,[22, 41-48] Klein,[42, 45, 46, 49-56] Luckham,[49, 51, 54, 55, 57] Fetters,[45-47, 52, 53, 56] and Claesson.[58-62] One application of the surface force apparatus is to study adsorbed polymers in conjunction with ellipsometry and adsorption studies. Since cell adhesion molecules are all polymers, a polymer physics method of investigating these molecules may improve the understanding of binding and dissociation. The following is a review of some of the advances in measuring the interaction between polymers.

Klein and Luckham have investigated the forces acting between poly(ethylene oxide) adsorbed onto mica surfaces in cyclopentane solution.[49] Using the SFA, they studied the interaction force while varying molecular weight, compression and decompression intervals, and approach and separation rates. The onset of the interactions between adsorbed polymers was measured at 3Rg, three times the radius of gyration. Klein and Luckham have also measured the interaction forces between mica surfaces immersed in toluene.[54] In this study, PEO and PS of molecular weight from 40 Kg/mol to 310Kg/mol were introduced into toluene. Following adsorption of the polymers, force-distances curves were measured. They found that in pure toluene, a good solvent for both PEO and PS, showed a short-range van der Waals attraction. Since toluene is a good

solvent, both PEO and PS are well solvated in solution, simulating proteins at the surface of cell membranes. In experiments involving nonspecific protein-protein binding, one may expect van der Waals attraction.

Claesson has worked with adsorption of copolymers of PEO and ethyl(hydroxyethyl)cellulose (EHEC). Hydrophobic surfaces (Langmuir-Blodgett films deposited on mica) were coated with EHEC (mw 250 Kg/mol), and the force was measured as a function of temperature in aqueous solution.[61] It was discovered that the force changed from repulsive to attractive as the temperature increased. The researchers explained this phenomenon by dividing the interaction force into two components: the elastic and the osmotic. The elastic interaction results from the loss of conformational entropy and volume for the polymer chains as the two surfaces approach. This elastic force is generally repulsive. The osmotic interactions come from the increase in polymer concentration as the two surfaces are brought together. For the osmotic interaction, if the Flory-Huggins interaction parameter, χ, is larger than 0.5, then the force is attractive, but if $\chi < 0.5$, then the force is repulsive. Attractive forces for $\chi > 0.5$ (when the polymer is essentially insoluble) can also be attributed to entanglement between adsorbed chains on the two surfaces. Cell adhesion receptors may be modeled as two polymer chains in solution. While the value of the χ parameter depends on the individual receptor, the osmotic interactions are likely to be negative since proteins are soluble.

All of the work described in the previous paragraph used a neutral solvent. When electrolytes are added to the experiment, another force becomes important. As the surfaces approach, the electric double-layer of ions adsorbed onto the surfaces creates a repulsive force. In one study, the researchers investigated the interactions between mica

surfaces in a pH 9.9 solution. The SFA showed repulsive forces between the mica when no polymer was present. When poly(ethylene imine) was added, there was a weak adhesive force upon separation of the surfaces. Claesson *et al*., attribute this attraction to bridging (the polymer chain is adsorbed upon both surfaces). Bridging effects may also be seen in the biological interactions investigated in this thesis.

Experimental Outline

In my thesis, I measured some of the adhesive forces between receptor-ligand pairs using the atomic force microscope. First, I measured the forces between biotin grafted onto silica microspheres and avidin grafted onto glass surfaces. To determine whether free biotin had any effect on the force of adhesion, I varied the concentration of free biotin in the measurements. Next, I measured the forces between sialyl Lewis X and selectin expressing endothelial cells. Selectins are adhesion molecules involved the tethering and rolling of leukocytes in flowing blood. I also initiated an investigation of how topography affects endothelial cell growth and adhesion to polydimethylsiloxane substrates. Porcine vascular endothelial cells were obtained from Dr. Edward Block's group in the Malcom Randall Veterans Adminstration medical center. Characterization of the cells was performed with the assistance of Dr. C. Keith Ozaki.

CHAPTER 2

BIOTIN-AVIDIN INTERACTION

Background

Biotin, commonly known as the water-soluble Vitamin H, is a cofactor in several enzymatic carboxylation reactions. Consequently, it is found in both tissue and blood. It has a molar mass of 244 g/mol and has a high affinity for both the bacterial protein streptavidin and the related egg-white glycoprotein avidin. The interactions between biotin and avidin/streptavidin form two of the strongest protein-ligand complexes known. The affinity of biotin for avidin is $K_a = 10^{13}$-10^{15} /M,[63] and the free energy of association is 21 kcal/mol. Usually, antibody-antigen interaction has an affinity of 10^7 -10^{11} /M. Though the strength of the bond is pH dependent, the bond is stable over a broad pH range. Thus, the biotin/streptavidin complex has been used as a model to study the molecular basis of ligand-macromolecule interactions. The high affinity of biotin for streptavidin has also been used in many bioanalytical techniques. Since the biotin/avidin system is common and well characterized by x-ray crystallographic and genetic techniques, I decided to investigate this system first. AFM force measurements of biological receptors in the inexpensive biotin/avidin system were stepping stone toward more complex systems. Also, although the forces between biotin and avidin have been measured previously,[64, 65] there are some issues with the data such that a modification in the sample preparation may generate new insights into how biotin binds to avidin. Before

discussion of the forces involved in binding, a discussion of the current knowledge about the structure and binding of streptavidin, avidin, and biotin is in order.

Structural Properties of Streptavidin and Avidin

Streptavidin is a tetrameric protein isolated from Streptomyces avidinii with a molecular weight of approximately 60 Kg/mol. Each subunit is folded into an eight-stranded antiparallel β barrel.[66-68] At one end of this barrel is the binding site for biotin. Thus, there are four binding sites for biotin per streptavidin. This binding site contains both amino acid residues from the interior of the barrel and that from a loop region attached to an adjacent subunit. Unlike many proteins composed of different subunits (i.e. hemoglobin), streptavidin does not exhibit cooperative binding.[69] The loop region of the adjacent streptavidin subunit encloses the binding pocket, so that once biotin is bound to the pocket of the barrel, it is not solvent accessible (Fig 2.1). The valeryl side chain carboxyl oxygens of biotin links to the side chain of Ser88 and the primary chain nitrogen of Asn49 through hydrogen bonds. The ureido ring forms hydrogen bonds to the side chain of Asp128 and, the side chain of Ser45 by the two primary amines. The side chains of Tyr43, Asn23, and Ser27 can also hydrogen bond to the carboxy on the ring. In addition to hydrogen bonding, the biotin molecule is bound through hydrophobic interactions. Four tryptophan residues, Trp79, Trp92, Trp108, Trp120, from an adjacent streptavidin subunit interacts with the tetrahydrothiophene ring of the biotin.[70] Due of all the hydrogen bonds and the hydrophobic interactions, the release rate of biotin from streptavidin is exceptionally slow.[71]

Biotin and avidin interact in a manner similar to biotin and streptavidin.[70, 72] Avidin, which is also a tetramer, is a glycoprotein and has a molar mass of approximately 67Kg/mol. The binding pocket in avidin also contains the aromatic side chain of Phe72, which interacts hydrophobically with the valeryl side chain of the biotin. The valeryl carboxyl group forms three hydrogen bonds in avidin, instead of two in streptavidin. Avidin also has a longer loop that closes over the binding site, making it less accessible to solvent. These differences most likely account for the higher affinity of avidin for biotin compared to streptavidin and biotin.

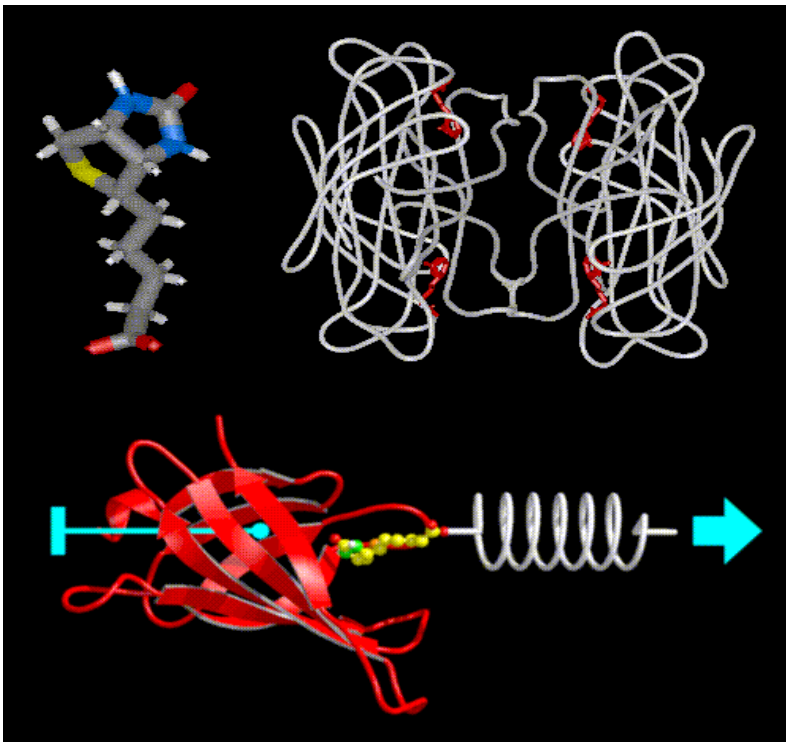

Figure 2-1. The top figure is a schematic of the avidin-biotin binding process, obtained from the web site of Dr. Helmut Grubmuller, http://www.mpibpc.gwdg.de/abteilungen/071/strept.html. The figure on the bottom left is a three-dimensional representation of avidin, and the figure on the bottom right, is a representation of biotin.

Binding Characteristics of Streptavidin

My work uses the AFM to measure the binding forces in the avidin/biotin system. Since the binding characteristics have been measured previously, a review of the literature is necessary. Weber and coworkers[66, 68, 73] have proposed that the exceedingly strong binding of streptavidin to biotin ($K_d = 10^{-15}$ M) is the polarizable carbonyl group of the ureido ring, which forms three hydrogen bonds in the binding site. From molecular dynamics and free energy calculations, Miyamoto and Kollman[74] state that van der Waals interactions are more important than electrostatic and hydrogen bonding interactions. By modifying the tryptophan residues from the enclosing loop (Trp79 and Trp108) through site-directed mutagenesis researchers have confirmed that van der Waals interactions are important. The mutated streptavidin had binding constants 10^6 lower than normal streptavidin.[75]

The atomic force microscope has been used to make direct measurements of the force required to rupture a single streptavidin-biotin bond.[64, 65] Florin, Moy, and Gaub determined the rupture forces between biotin and avidin by physisorbing biotinylated bovine serum albumin (BSA) to the tips of AFM cantilevers.[64] Then, the AFM tip was incubated with avidin, and force measurements were taken against biotinylated agarose beads. Thus, for these experiments, the total measured force involves the physical adsorption of BSA, the binding of the BSA-biotin to avidin, and another binding of avidin to biotin on an agarose bead. The agarose bead yields when pressed by the cantilever, increasing the total sum of interactions that occur between the tip bound avidin and the surface bound biotin. Therefore each force curve is composed of the interactions of many biotin-avidin pairs. Hence, the quantized force of interaction for a single pair

must be determined through an autocorrelation analysis. Using this analysis, the calculated force required to rupture a single biotin-avidin pair is 160 ± 20 pN. To confirm this measurement, Florin *et al* measured the binding force after the addition of free avidin to the fluid cell. The free avidin reduced the overall adhesive force, but did not change the calculated force of a single biotin-avidin pair. The free biotin also reduced the number of binding contacts.

Florin *et al*.[64] also measured the force between avidin and desthiobiotin and iminobiotin, two analogs that have lower binding constants than biotin. They calculated a binding force of 125 ± 20 pN with desthiobiotin, and 85 ± 15 pN with iminobiotin. Later, the same group[65] compared the unbinding or rupture force of five different avidin-biotin pairs with corresponding thermodynamic energies. The dissociation force required to separate the bound compounds varied from 257 ± 25 pN for streptavidin-iminobiotin to 85 ± 10 pN for avidin-iminobiotin. There was no correlation between the free energy, ΔG, and the dissociation force, but there is a direct proportionality between the enthalpy and the dissociation force. The proportionality factor was christened the effective width of the binding potential, $r_{eff} = \Delta H/F_{dissociation}$, which was 95 ± 10 nm. Moy, Florin, and Gaub[65] then suggested a model for ligand-receptor dissociation based on the free energy and enthalpy of the process that explains the correlation between the enthalpy and the dissociation force.

The structural analysis of avidin/biotin binding from X-ray crystallography gives a general view of how biotin fits into avidin the classic lock-and-key model, but a more rigorous kinetic (and thermodynamic) model is necessary to fully explain ligand binding. Thus, atomic force microscope was used to measure the rupture force between biotin and

the forementioned tryptophan mutants (at Trp79, Trp108, and Trp120).[75] The rupture force was correlated with changes in equilibrium thermodynamic parameters (free energy, enthalpy), and the activation thermodynamic barriers for the dissociation of the biotin-streptavidin complex (free energy of dissociation, and enthalpy of dissocation). A correlation existed only with the activation enthalpy of dissociation.[75] To determine the mechanism of unbinding, Grubmuller, Heymann, and Tavan used molecular mechanics calculations.[76] The computer simulation suggested a multiple-pathway rupture mechanism, which involves five major unbinding steps, each corresponding to the break of hydrogen bonds.

As stated earlier the binding forces between biotin and avidin have been measured by Florin, Moy, and Gaub.[64, 65] There are several issues with their method of using biotin that was physically adsorbed to the AFM tip. First, the measurement of forces by AFM quantifies the weakest force available. Thus, if the force to rupture the bond between avidin and biotin is stronger than the force to take the adsorbed biotin off the AFM tip, then the force reported would be the force of adsorption. Since the avidin-biotin bond is the strongest non-covalent bond in biology, this possibility cannot be ignored. I circumvented this issue by covalently linking the biotin to microspheres bonded to AFM tips. I also added a spacer molecule, poly(ethylene glycol) of MW = 3,400 Da, between the biotin and the microsphere. This spacer allowed the biotin to be mobile, and thus bind effectively with avidin. The calculation to convert the AFM data to a force-distance graph is also different in my method. Florin *et al.*[64] did not account for the radius of the tip by normalizing the value for the force to force per area. Thus, any variation in the tip radius would affect the result. This study uses the Derjaguin approximation between a

rigid sphere and a flat surface to normalize the force. To perform the normalization, one must measure the radius of the tip, which was performed with scanning electron micrographs of the glass microsphere bonded onto the AFM tip.

Materials and Methods

Previously, Florin, Moy, and Gaub attached biotin to AFM tips by non-specifically adsorbing biotinylated BSA.[64] The biotinylated BSA may desorb in solution, which would render the force measurements useless. So in the following experiments, the biotin is covalently bonded to a microsphere through 3-aminopropyltriethoxysilane and polyethylene glycol (PEG) of 3.4 Kg/mol. Thus, there is a spacer, the PEG, between the biotin and the microsphere, which allows the biotin the mobility to bind with avidin. The microsphere is then bonded to the AFM tip using epoxy. A micromanipulator is used to physically place the epoxy and the microsphere onto the AFM tip. A micromanipulator is an instrument that allows minute movements in the x, y, and z axes. Attached to one end of the micromanipulator are thin tungsten filaments. Using one filament, the operator can deposit the epoxy glue onto the AFM tip, and then, using another filament, pick up a microsphere and place it onto the tip.

Grafting of 3-Aminopropyltriethoxysilane on Glass

A silane coupling agent, 3-aminopropyl triethoxysilane (APS), was grafted to glass. First, the glass was cleaned ultrasonically for five minutes in a chloroform and methanol solution and then dried in air. A solution of dry toluene and APS were combined in a round bottom flask and allowed to mix before addition of both the glass

microspheres and the glass slides. After the addition of the microspheres and the slides, the solution was stirred before heating to the desired temperature. The reaction proceeded at temperature for 12 hours after which time the wafers were removed, and rinsed with toluene. To fully condense the APS, the glass was dried and placed in an oven at 110 °C for 1 hour. The efficacy of this procedure was confirmed using x-ray photoelectron spectroscopy (XPS) (Table 2.1).

Table 2.1. XPS data of plain glass and APS grafted glass. The increase in nitrogen and carbon indicates grafting of the silane coupling agent.

Element	Plain glass (Mass Conc%)	APS grafted glass (Mass Conc%)
C1s	15.3	31.1
O1s	46.0	34.1
Si2p	38.9	30.1
N1s	00.0	04.7

Limitations of the XPS only allowed characterization of glass slides, and not the glass microspheres used in the experiment. However, given the same composition of both slides and microspheres, and the same reaction used in both, one may state that the successful grafting of the slides mean success for the microspheres.

Biotin Grafting to Glass

After the glass was treated with APS, I added biotin to the surface. I obtained ω-N-hydroxysuccinimidyl ester of poly(ethylene glycol)-carbonate, MW = 3400 g/mol, from Shearwater Polymers (Huntsville, AL). Hereafter, this material will be referred to as NHS-PEG-biotin.

Characterization of Biotin Grafted Surfaces

Avidin is the conjugate for biotin in biology. We used the natural affinity between biotin and avidin to measure the concentration of biotin on the surface. ExtrAvidin®-FITC conjugate, which absorbs at 280 nm and 495 nm, was purchased from Sigma-Aldrich (St. Louis, MO). Fluorescein isothiocyanate (FITC), is a common fluorescent dye attached to proteins that is used to identify the presence of those proteins. Four samples were investigated. First, to detect autofluoresence, both the control, a glass slide that had been reacted with APS only and the test sample, which was a glass slide grafted with biotin, were photographed using a Zeiss fluorescent optical microscope at 10X magnification. All pictures were exposed for 1.5 seconds, and the relative intensities were measured (Figure 2-2a). Then the ExtrAvidin®-FITC conjugate was added to both the test sample and the control, and then washed with deionized (DI) water(Figure 2-2b). The test sample increased in fluorescence, thus showing that the biotin had been successfully grafted onto the surface of glass slides.

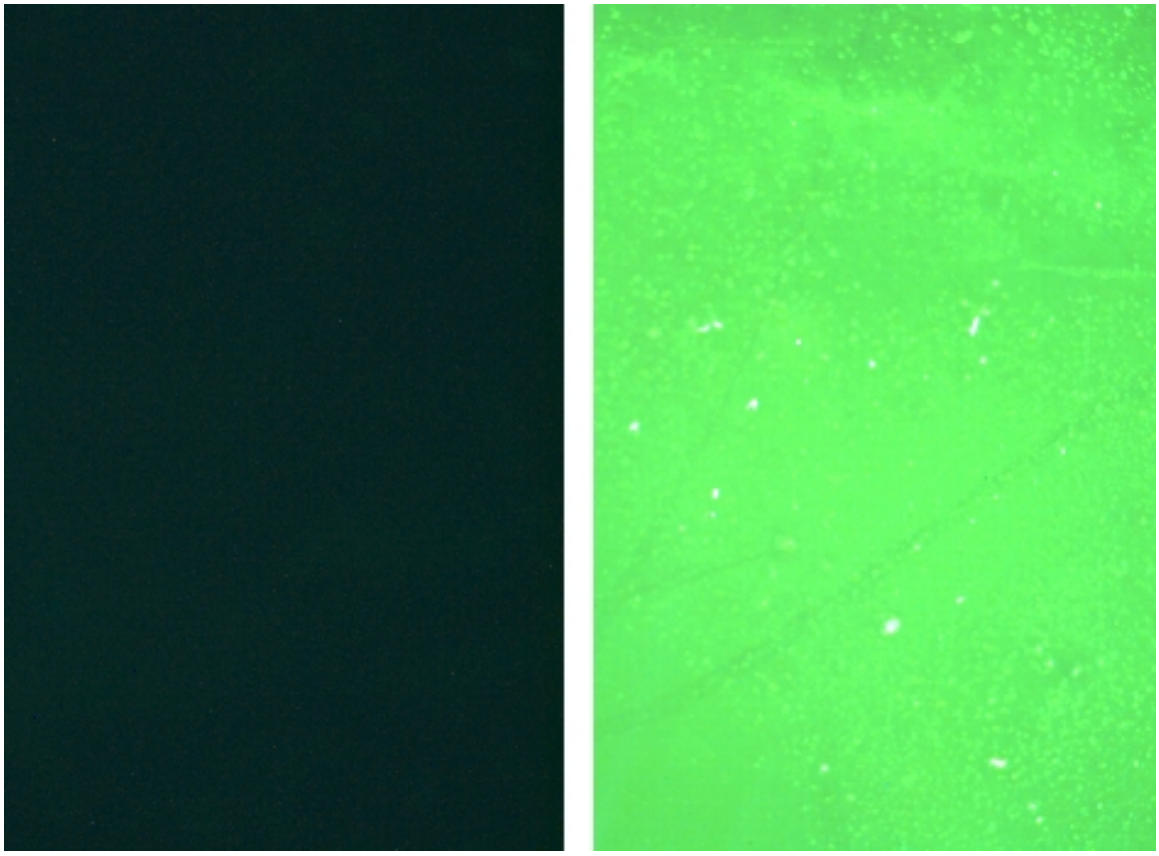

Figure 2-2. The picture on the left shows a plain glass surface that had been dipped in ExtrAvidin -FITC, and then washed with PBS. The picture on the right shows a biotinylated glass surface, dipped in ExtrAvidin -FITC, and then washed with PBS. The increase in color indicates specific binding of the avidin to the biotin on the surface.

Attachment of Avidin to Glass Slides

To attach avidin to glass, APS and glutaraldehyde were first grafted onto the glass to provide the correct reactive functionalities. The treatment with APS is the same as outlined above. Then, an 8 % glutaraldehyde solution in phosphate buffered saline (PBS) at pH of 7.4 was added to the APS grafted glass slides. The mixture was left overnight with end-to-end mixing. The glass slides were removed from the glutaraldehyde and washed (4X) with PBS. Some 0.05 % avidin-FITC was added to the glutaraldehyde

treated glass slides. As before, a fluorescent optical microscope was used to identify that avidin was attached to the glass (Figure 2.3).

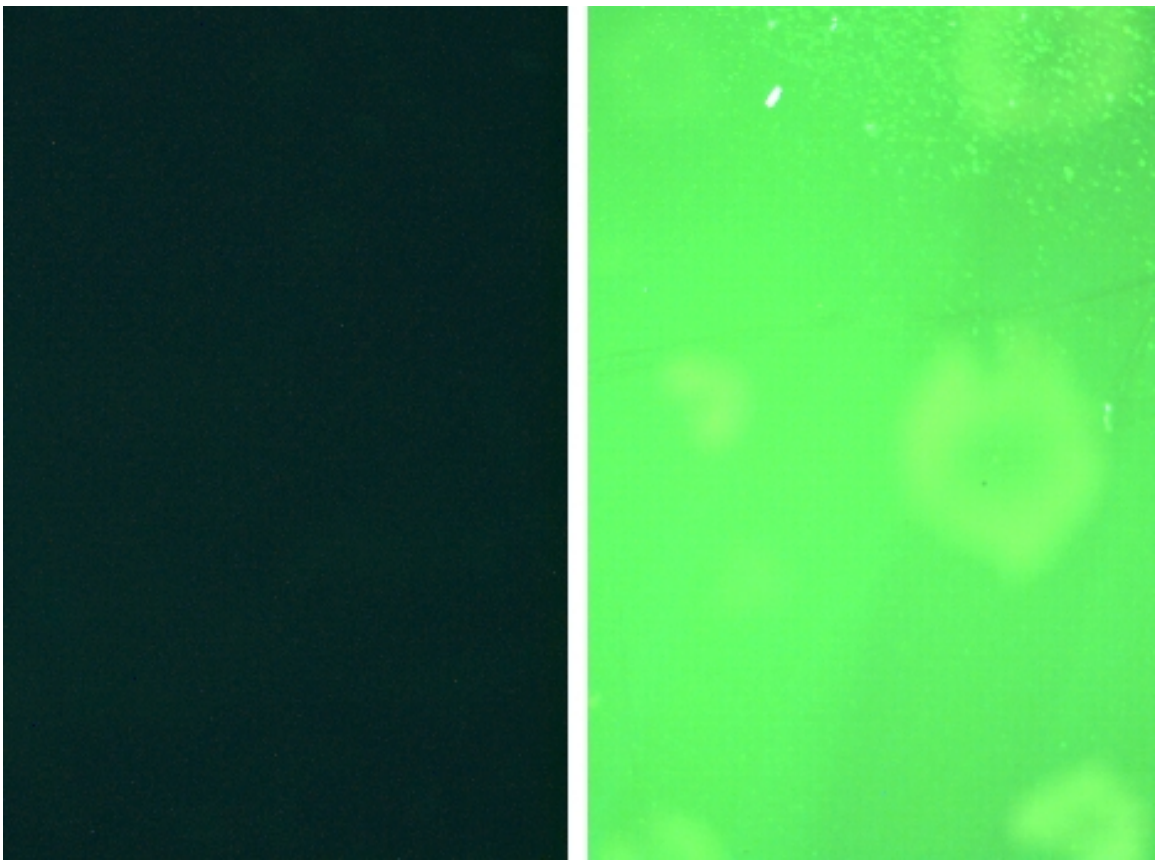

Figure 2-3. The picture on the left is a glass surface reacted with glutaraldehyde, but no ExtrAvidin -FITC. There was no autofluorescence. The picture on the right was reacted with glutaraldehyde and ExtrAvidin -FITC, and washed 3 times in PBS. The increase in intensity is indicative of the successful reaction of avidin onto the glass surface.

Atomic Force Microscopy

Force measurements were done on a Digital Instruments Nanoscope III atomic force microscope. The experiment was conducted inside a fluid cell provided by the manufacturer. The fluid cell allows the solution in the cell to be changed without disturbing the experimental setup. AFM tips modified with biotin were brought into contact with three different samples. First, plain glass slides without any modifications

were used. Next, glass slides modified with glutaraldehyde were used. Then, force measurements were taken using glass slides with avidin grafted to the surface. Ten measurements were taken for each substrate. To calculate the adhesion force and the interaction energy, the radius of the particle was determined by optical microscopy and scanning electron microscopy (Figure 2-4). The spring constant, 0.12 N/m for the tip was obtained from the manufacturer (Digital Instruments, Santa Barbara, CA).

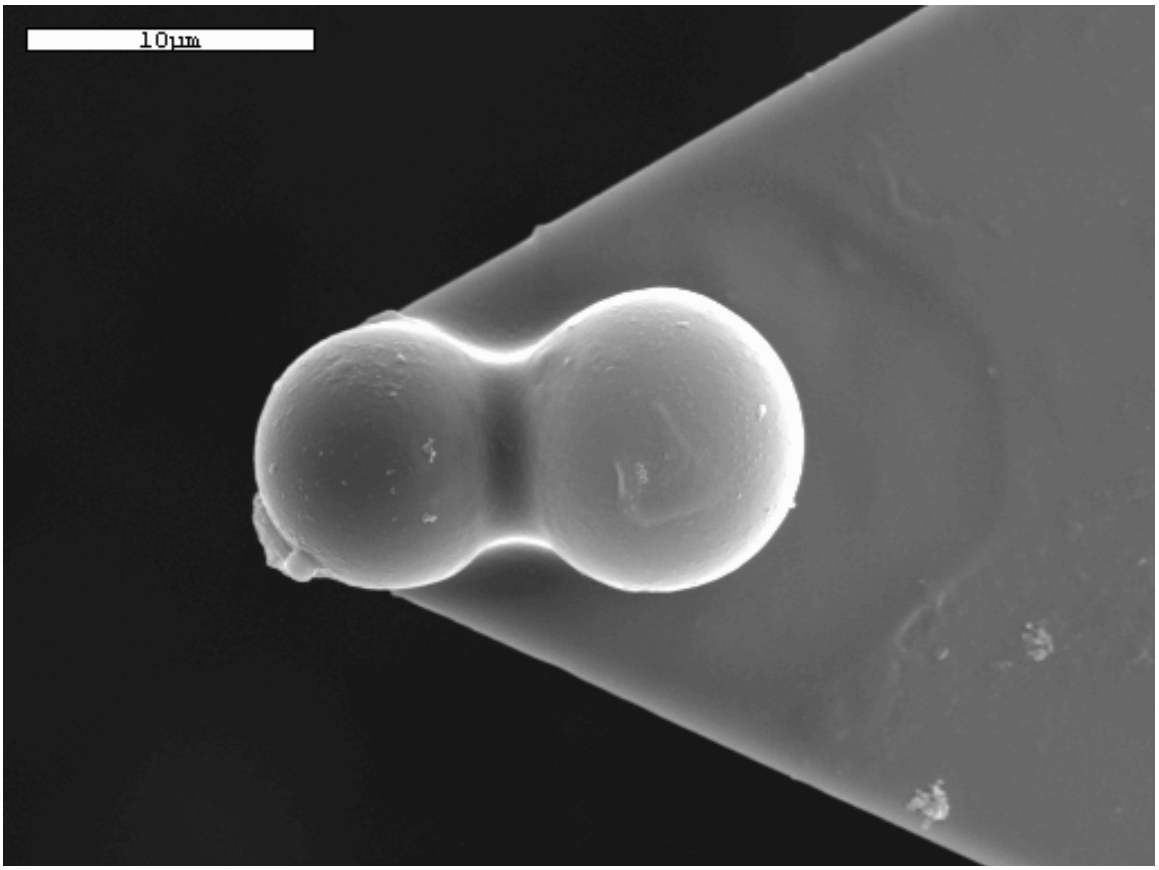

Figure 2-4. Occasionally, the microspheres are different than anticipated. Here, the experimenter accidentally bonded a doublet to the AFM cantilever. The microsphere was reacted with APS and PEG-biotin.

Effect of Concentration

Force measurements were also performed with three different concentration of biotin in PBS (0.5 %, 1 %, and 2 %). Ten measurements were taken for each substrate, with the appropriate solution of biotin in the AFM fluid cell. Free biotin may act as an inhibitor by binding to the avidin. Thus the force of adhesion that is measured between the biotin and avidin may decrease with the addition of free biotin.

Results and Discussion

Using the Derjaguin approximation, the forces between the biotin grafted AFM tip and the glass surface were normalized to the radii of the microsphere. The forces between biotin and the plain glass resulted in -0.24 ± 0.08 nN/μm. The forces between biotin and glutaraldehyde grafted glass were significantly larger ($p = 0.001$). The increase in the attractive force between biotin and glutaraldehyde may be attributed to hydrogen bonding with the glutaraldehyde. The plain glass is a flat surface whereas the addition of APS and glutaraldehyde creates a carpet of hydrophilic groups than can attract the biotin molecule. The interaction between biotin and avidin was both significantly larger ($p = 4.63$ E -05) and occurred at a significantly greater distance ($p = 6.36$ E -06) than that between biotin and glutaraldehyde. The increase in both the distance of interaction and the force is due to the specific binding with the biotin by the avidin grafted to the surface (Table 2-2).

Table 2-2. Force measurements between biotin grafted microspheres and three substrates

Microsphere	Biotin-PEG	Biotin-PEG	Biotin-PEG
Substrate	Glass	Glutaraldehyde-glass	Avidin-gluteraldehyde-glass
Distance(nm)	40.5 ± 14.0	46.0 ± 14.5	116.5 ± 26.9
Force (nN/μm)	-0.24 ± 0.08	-0.53 ± 0.16	-0.96 ± 0.15

The force measurement was also performed with varying concentrations of biotin in solution (Table 2-3). I had expected the biotin to block the binding sites of the avidin, and thus, reduce the force. There appears to be no variation in the distance or the strength of the force with changing concentration.

Table 2-3. Force measurements with different concentrations of free biotin in solution.

Biotin Concentration	0 wt%	0.5 wt%	1.0 wt%	2.0 wt%
Distance (nm)	116.5 ± 26.9	83.5 ± 24.2	84.0 ± 23.3	91.0 ± 22.2
Force (nN/μm)	-0.96 ± 0.15	-0.99 ± 0.27	-0.95 ± 0.20	-0.94 ± 0.15

A t-test was performed between the three samples. There was no significant difference in distance or force between the 0.5 %, 1.0 %, and 2.0 % concentrations. Differences from force measurements performed without free biotin in solution were also tested statistically (Table 2-4). One explanation for this result is that the concentration of biotin was not sufficient to cause a significant blocking of the binding sites on avidin. Another possibility is that the biotin adsorbed onto the surface of the substrate, and thus, did not bind to avidin. To fully explain why the addition of biotin did not affect the force measurements, more experiments must be performed. First, higher concentrations of free biotin should be used. Perhaps a critical concentration must be reached to block the binding. Biotin may adsorb to the glass surface. Thus, a different, preferably

hydrophobic, surface grafted with avidin may be used to determine if biotin adsorption is affecting the force measurements.

In summary, the force measurements conducted with biotin-PEG grafted microspheres with the plain glass showed a difference in binding between that of the plain glass, the glutaraldehyde modified surface, and the avidin grafted surface. The increase in attraction between the avidin grafted surface and the biotin grafted microsphere may be attributed to the specific receptor ligand binding. When free biotin was added to solution, no significant effect on the interaction is found.

Table 2-4. List of p-values for t-tests. The first value in each box, P_D is for comparisons of the distances, and the second value, P_F is for comparisons of the force measurements

	0.5 %	1.0 %	2.0 %
0.5 %	N/A	$P_D = 0.96$ $P_F = 0.68$	$P_D = 0.48$ $P_F = 0.59$
1.0 %	$P_D = 0.96$ $P_F = 0.68$	N/A	$P_D = 0.50$ $P_F = 0.92$
2.0 %	$P_D = 0.48$ $P_F = 0.59$	$P_D = 0.50$ $P_F = 0.92$	N/A
0 % biotin, interaction of biotin and avidin	$P_D = 0.0023$ $P_F = 2.69E-07$	$P_D = 0.0018$ $P_F = 1.61E-08$	$P_D = 3.08E-04$ $P_F = 5E-10$
Biotin and glutaraldhyde	$P_D = 3.23E-08$ $P_F = 9.88E-08$	$P_D = 3.62E-04$ $P_F = 2.69E-07$	$P_D = 4.24E-05$ $P_F = 9.94E-06$
Biotin and glass	$P_D = 5.27E-04$ $P_F = 1.59E-04$	$P_D = 1.24E-04$ $P_F = 4.5E-09$	$P_D = 9.60E-06$ $P_F = 1E-10$

Future Work

The technique of measuring forces between receptor and ligand using AFM may be applied to other systems. As reported in the next chapter, this has already been performed with the selectin-sialyl Lewis X system. Modification to the biotin-avidin system may also be performed and investigated using this technique. For example, iminobiotin and desthiobiotin are two biotin analogs that bind less effectively to avidin. The forces between these two ligands and avidin may be investigated using the same techniques presented here. The changes in the force may be correlated to changes in binding affinity.

CHAPTER 3

SELECTIN-SIALYL LEWIS X INTERACTIONS

Background

In the previous chapter, I investigated the forces of adhesion between avidin and biotin, a system that had been extensively investigated. Avidin-biotin binding is not particularly relevant clinically, however. Thus, another system should be investigated. In this chapter, I will provide some background on cell adhesion molecules, and then focus on selectin mediated leukocyte rolling. Cell adhesion molecules are important for many processes, such as the growth of tumors, the function of the immune system, and reaction to biomaterials such as neointimal hyperplasia. One particularly important process is the attachment, adhesion, and diapedesis of leukocytes at sites of tissue injury. In the inflammatory response, leukocytes identify and bind to the site of injury via the combination of selectins and integrins. Upon activation by the injury, endothelial cells express E- and P-selectins, which are adhesion receptors that recognize carbohydrate ligands. These selectins weakly bind leukocytes in a process known as "rolling."[6] Following the initial binding by the selectins, integrins strongly bind leukocytes to the blood vessel wall. This process of leukocyte rolling and adhesion is the focus of my research. In the literature there is a dearth of work detailing direct force measurements of selectin binding.

Discussion of force measurements should be prefaced by a review of the biological behavior of selectins. In the past 20 years, three types of selectins have been identified: L-, P-, and E-.[4] L-selectins, the first to be discovered, are expressed by leukocytes. This form of selectin participates in the adherence of leukocytes to peripheral lymph nodes, and the recruitment of neutrophils and monocytes to inflammatory sites. P-selectins were discovered by investigators interested in platelet activation,[5] and is rapidly distributed to the surface of platelets upon activation by thrombin and other mediators. E-selectins are found on the endothelium, and support the adhesion of eosinophils, neutrophils, and monocytes.

Since selectins are important for the mediation of leukocyte rolling, they are important in the overall immune system. For example, patients with AIDS or leukemia often have elevated levels of serum L-selectin.[77] Another disease, leukocyte adhesion deficiency II, involves recurrent bacterial infections, and the dysfunction of neutrophil motility due to the lack of sialyl Lewis X.[78] Selectins have also been associated with injury due to ischemia and reperfusion,[79] and wound repair.[80] Sialyl Lewis X is even important for normal brain development,[81] as reported by Santos-Benito *et al*.

A complex cascade of interactions controls the binding of leukocytes. Chemokines[82] and platelet-activating factor[83] expressed on the endothelial cell surface are recognized by leukocytes after the initial contact. In contrast to most cell adhesion phenomenon, the recruitment of leukocytes from the flowing bloodstream is a very rapid process, which requires a special mechanism for the establishment of cell contacts. The selectins, which are distributed exclusively in leukocytes and the vasculature, are specialized for this purpose.

Selectin Composition

To understand why selectins exhibit this behavior, a review of the literature on the structural composition of the selectins in needed. The extracellular part of all selectins is composed of three different kinds of protein domains. The amine terminus of each selectin is a 120 amino acid domain that has features similar to C-type animal lectins, so called because the binding of carbohydrates is dependent on the presence of extracellular calcium.[84] This domain is followed by a sequence of ~35-40 amino acids similar to a repeat structure originally discovered in epidermal growth factor (EGF). The single EGF domain is followed by several "complement binding" (CB) domains, containing ~60 amino acids. Patel, Nollert, and McEver[85] showed that reducing the number of CB domains in P-selectin decreases the efficiency of rolling, which suggests that these CB domains are involved in the extension of P-selectin a sufficient length from the plasma membrane. Size differences between the types of selectins and between animal species involve different number of CB domains. For example in rats, the E-selectins have five CB domains and the P-selectins have eight, while in humans, E- and P-selectins have six and nine respectively. L-selectins in both species have only two CB domains.[86] All of the selectins are anchored in the membrane by a transmembrane region followed by a short cytoplasmic tail (Figure 3-1).

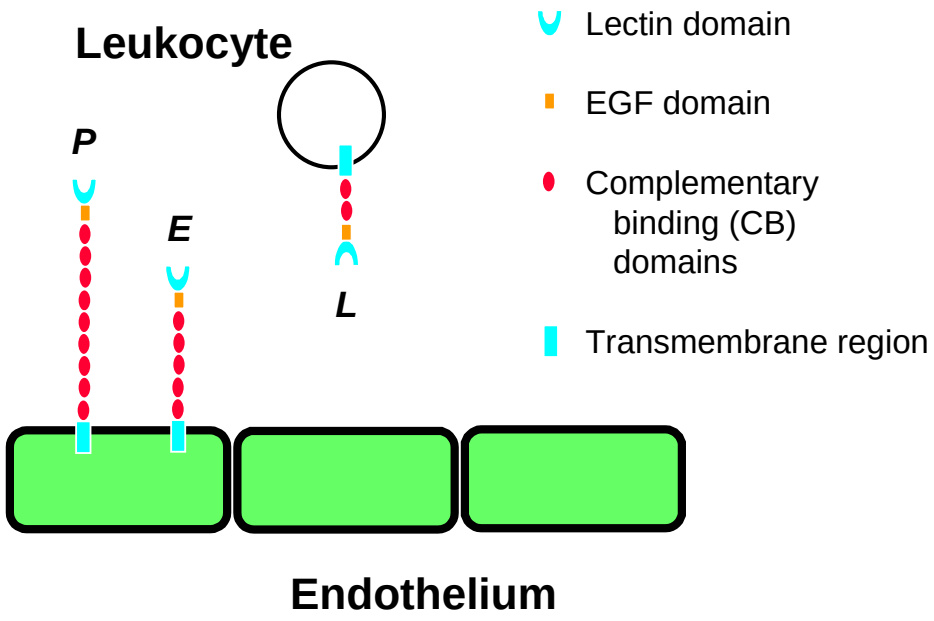

Figure 3-1. Schematic of three kinds of selectins in humans

Since contact between most leukocytes and endothelium is initiated by selectins, their regulation is important for control of diapedesis. E- and P-selectins are only present on the surface of endothelium activated by proinflammatory stimuli. Thus, leukocyte rolling will only occur in inflamed tissues. L-selectins are constitutively expressed on leukocytes. E-selectin is induced by cytokines such as interleukin-1-β and tumor necrosis factor-α and lipopolysaccharide in human umbilical vein endothelial cells.[87, 88] Some 3-4 hours after activation, maximal levels of E-selectins are expressed on the surface. P-selectins are stored in α-granules inside platelets, and in Weibel-Palade bodies in endothelial cells. They are rapidly mobilized after stimulation with histamine or thrombin.[89] Expression is maximal at ~5-10 minutes, and is cleared from the surface with 60 minutes. This regulation may be an important avenue for future research. Conceivably, force measurements may be performed on cells in varying environments. Thus, a study of how selectin expression affects the forces measured may be conducted.

Biophysical Parameter of Selectin-Ligand Interaction

Since this study involves measurements of the forces of specific receptor-ligand interaction, a discussion of previous attempts at measuring the selectin-SLe^X bond is necessary. Based on the leukocyte rolling assumption, selectins have been proposed to have rapid rate constants for bond association and dissociation, and special mechanical properties for tensile forces and bond dissociation.[90-92] Also, the affinity of selectins for their ligands does not need to be especially high. Several groups[93-98] had measured binding between selectins and the tetrasaccharide sialyl Lewis X or its stereoisomer sialyl Lewis A to be fairly weak (dissociation constant K_d = 0.1-5 mM). Binding kinetics between the interaction of L-selectin and its ligand, glycosylation-dependent cell adhesion molecule-1 (GlyCAM-1) has also been determined.[99] The authors showed that L-selectin binds to GlyCAM-1 with a K_d of 108 μM, and dissociates very fast, with a dissociation rate constant k_{off} of ~10 s^{-1}. Other studies with P-selectin and P-selectin glycoprotein ligand-1 (PSGL-1) revealed a K_d of 200 nM, and a k_{off} of ~1.5 s^{-1}.[100]

Other than fast association rates, high tensile strength of the selectin-ligand bond was suggested to support the rolling function.[101] Using a laminar flow chamber, the experimenters visualized tethering and release of neutrophils on lipid bilayers containing incorporated P-selectin. Flow subjects leukocytes to a shear force that increases the k_{off}, in the absence of shear, an "intrinsic k_{off}" was determined by extrapolation to zero flow rate. By analyzing the kinetics of the transient binding events (tethers), Alon, Hammer, and Springer[101] showed that the intrinsic k_{off} for P-selectin as 1 s^{-1}. The bond interaction distance was determined to be 5 nm. An intrinsic k_{off} of 7 s^{-1} was determined with similar measurements for L-selectin, using L-selectin expressing neutrophils flowing over

substrates coated with L-selectin ligand.[102] L-selectin mediated rolling appears to be faster than rolling mediated by E- or P- selectin, which agrees with the observation that the k_{off} of L-selectin is ~10 s^{-1} higher than that for E- and P-selectins.[103-105] The faster rolling of leukocytes on L-selectins may also be explained by the fewer number of CB domains. As stated earlier, the CB domains are involved in the extension of the selectin away from the membrane. Thus, the shorter L-selectin does not extend as much, which leads to decrease time of interaction, and faster rolling.

Selectins are not the only molecules that support leukocyte rolling. Using in vitro adhesion assays under flow, tensacin,[106] vascular cell adhesion molecule-1, a4b7/mucosal addressin cell adhesion molecule-1,[107] and CD44/hyaluronan[108, 109] also allowed rolling. Selectins are much more efficient at this task, however. For example, when the differences between leukocyte rolling on immobilized antibodies versus Le^X and SLe^X was examined,[110] antibodies supported rolling only within a small range of site densities and wall shear stresses, while the selectin mediated rolling occurred throughout a wide range. For example, the antibody PM-81 showed leukocyte rolling at a site density of 100-150 sites/μm^2, a wall shear stress of 0.5 to 8.0 dyn cm^{-2}, and a velocity of 0.2 to 0.6 μm/sec. For leukocytes rolling on E-selectin, the range was 35-900 sites/μm^2, 0.5 to 32.0 dyn cm^{-2}, and a velocity of 1.3 to 10 μm/sec. Shear stress above a critical threshold is required to maintain rolling interactions in L-, E-, and P-selectins.[111,112] It has been suggested that the fluid shear may induce additional bond formation by deforming the cell slightly after the first bond forms, thus increasing the time and area of the cell/substrate contact. Taylor and coworkers developed a technique to explain the transition from tethering to adhesion.[113] Using a cone-plate viscometry, they showed that the binding

kinetics of selectin and integrin are optimized to function at discrete shear rate and stress. Thus, the leukocyte recruitment process requires specific flow rates and receptor densities. Although this study measured forces in a static fluid chamber, future work may involve measuring the adhesion at varying flow rates and receptor densities.

Selectin Ligands

The ligands for the selectins are also important for a basic understanding of the rolling process. Instead of the ligand binding through protein-protein interactions found on most cell adhesion molecules, the ligands of the selectins bind with carbohydrates attached to either a scaffold protein or a lipid carrier molecule. By itself, the carrier molecule is insufficient to define a selectin ligand—it must be expressed in the correct cellular environment to allow glycosylation (attachment of the carbohydrate moiety).

Oligosaccharides can bind to selectins on several different molecules, even ones not used as carriers physiologically. For example, BSA has been used as to bind selectins.[114,115] Also, oligosaccharides are not the only modifications required to make a carrier molecule capable of binding selectins. For example, tyrosine sulfonation is also required to make PSGL-1 able to bind to selectins.[116-118]

Both glycolipids and glycoproteins can act as carriers for sialyl Lewis X. Glycolipids carrying oligosaccharides such as sialyl Lewis X have been shown to support rolling of E-selectin transfected cells, and of L-selectin expressing leukocytes.[119] PSGL-1 was identified by expression cloning,[120] and by affinity isolation as a 250-kDa disulfide-linked dimer.[121] It is the only ligand so far that has been demonstrated, *in vivo*, to mediate leukocyte rolling on endothelium,[122] and leukocyte diapedesis into inflamed

tissue.[123,124] This ligand is widely expressed in cells of lymphoid, dendritic, and myeloid linkage.[125] Thus, every leukocyte has PSGL-1. While the model system used in this study does not involve PSGL-1, the BSA used in the experiments effectively simulates the function of the PSGL-1.

Hypothesis

The characteristics of selectins that allow leukocyte rolling are distinctive. Selectins are cellular brakes: they must attach quickly, bind weakly, and then release the ligand. Under flow, fast interactions between selectin and ligand are essential because leukocytes are rushing past the endothelium. They must also bind weakly, otherwise, either the selectin or the ligand will be torn out of the cell membrane by the momentum of the leukocyte. To investigate the nature of the forces of adhesion between selectins and ligands, we have chosen to use Atomic Force Microscopy (AFM). The movement of the AFM cantilever effectively simulates the rolling process. The initial contact between the ligands on the leukocyte and the endothelium is reproduced when the tip is extended onto the cell membrane. At this time, the sialyl Lewis X binds to the selectin on the endothelial cell surface. The retraction of the AFM tip simulates the rolling of the leukocyte along the endothelium. As the leukocyte rolls, the ligand-receptor binding of SLe^X to selectin will be broken. The same occurs when the AFM tip retracts. During retraction, the AFM will measure the force required to pull a selectin to full extension, and the break the binding between SLe^X and the selectin. The understanding of this how leukocytes roll may be applied toward improved pharmaceuticals—drug delivery devices that target inflamed areas with blood vessels that express selectins.

Materials and Methods

SLe^X covalently linked to bovine serum albumin (BSA) was grafted onto silica microspheres (r = 5μm) using glutaraldehyde and 3-aminopropyltriethoxysilane (APS). Microspheres with BSA grafted directly onto the surface served as control for nonspecific interactions. The microspheres were bonded to AFM cantilevers. Porcine vascular endothelial cells (ECs) were grown using cell culture techniques on radiofrequency plasma treated polydimethylsiloxane elastomer substrates. Ten independent observations were made on test samples and controls as they were brought into contact with selectin expressing ECs. The Derjaguin approximation between spheres and flat plates was used to normalize force values.

Grafting of 3-Aminopropyltriethoxysilane on Glass Slides and Glass Microspheres

A silane coupling agent, 3-aminopropyl triethoxysilane (APS), was grafted to glass. First, the glass was cleaned with five-minute sonicating wash using chloroform and methanol. After the wash, the glass was dried in air. A solution of dry toluene and silane coupling agent were combined in a round bottom flask and allowed to mix before addition of the silicon wafers. After the addition of the wafers, the solution was allowed to stir before heating to the desired temperature. The reaction proceeded at temperature for 12 hours after which time the wafers were removed, and rinsed with toluene. To cure the silane coupling agent, the glass was dried and placed in an oven at 110 °C for 1 hour. The same procedure was performed in Chapter 2. The efficacy of this procedure was confirmed using x-ray photoelectron spectroscopy (XPS) (Table 2-1).

Limitations of the XPS only allowed characterization of glass slides, and not the glass microspheres used in the experiment. However, given the same composition of both slides and microspheres, and the same reaction used in both, one may state that the successful grafting of the slides mean success for the microspheres.

Addition of Glutaraldehyde

An 8 % glutaraldehyde solution in phosphate buffered saline (PBS) at pH of 7.4 was added to the APS grafted microspheres. The mixture was left overnight with end-to-end mixing, which allowed the aldehyde groups to react with the primary amine on the APS.

Addition of BSA-SLe^X or BSA

Some 0.01 % of SLe^X-BSA, purchased from Oxford GlycoSciences, Ltd (Oxford, England), in PBS was added to the glutaraldehyde/microsphere mixture. For the control samples, 0.01 % BSA was added to the glutaraldehyde modified microspheres. Carboxylic acid functional groups on the BSA react with the glutaraldehyde to covalently link the SLe^X to the microsphere. After the modification, the microsphere was bonded to the large, thick AFM cantilevers on contact mode tips. The microsphere is then bonded to the AFM tip using epoxy. A micromanipulator is used to physically place the epoxy and the microsphere onto the AFM tip. A micromanipulator is an instrument that allows minute movements in the x, y, and z axes. Attached to one end of the micromanipulator are thin tungsten filaments. Using one filament, the operator can deposit the epoxy glue onto the AFM tip, and then, using another filament, pick up a microsphere and place it

onto the tip. See Figure 3-2 for scanning electron micrographs of the AFM tip with the SLe^X modified tips. XPS was also performed on microspheres modified with glutaraldehyde, and BSA to demonstrate the efficacy of the reactions (Table 3-1).

Table 3-1. Comparison of XPS data from plain glass, glass modified with glutaraldehyde, and glass reacted with bovine serum albumen (BSA).

Element	Plain Glass (Mass Conc%)	Glutaraldehyde-APS-Glass (Mass Conc%)	BSA-Glutaraldehyde-APS-Glass (Mass Conc%)
C1s	15.3	31.1	57.6
O1s	46.0	40.2	28.6
Si2p	38.9	21.3	00.0
N1s	00.0	07.5	13.8

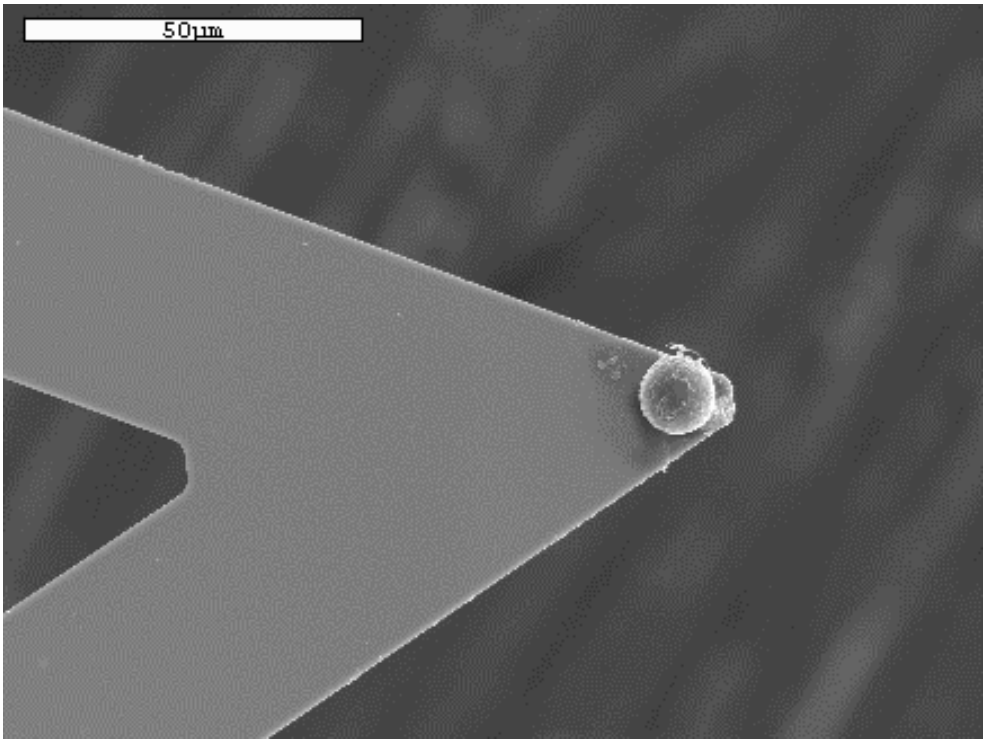

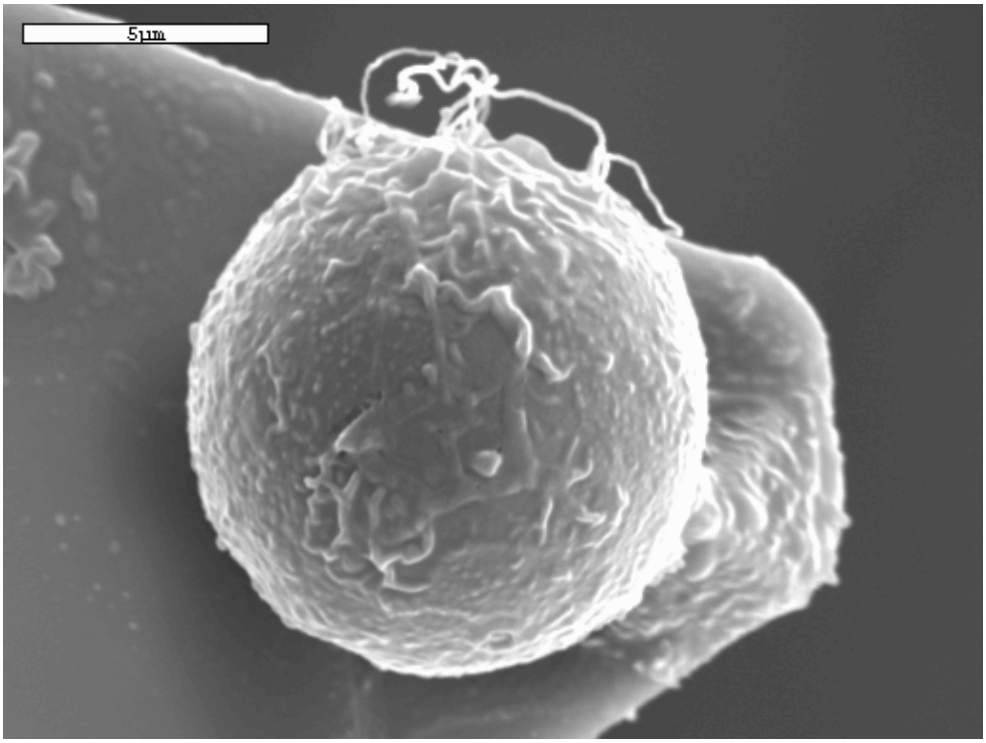

Figure 3-2. Scanning Electron Micrographs of SLeX grafted microspheres on AFM cantilevers.

Cells Grown on PDMS Substrates

T-2 Silastic silicone elastomer resin and base were obtained from Dow Corning. The exact composition of the T-2 Silastic is proprietary, but the basic components of vinyl functionalized PDMS, and a platinum crosslinking agent are present. The base and the resin are mixed together in a 10:1 ratio, degassed in a vacuum, and cast on silicon substrate for 24 hours.

Plasma Treatment of PDMS Substrates

PDMS substrates were treated by radio frequency glow discharge plasma. Using a RF Plasma Inc. HFS 401S instrument, set at 50 watts, the PDMS samples were plasma treated under 40 mTorr of vacuum in Argon for 5 minutes. This treatment created hydrophilic groups on the hydrophobic PDMS.

Porcine Vascular Endothelial Cell (PVEC) Culture

PVECs were obtained from Dr. Edward Block's group. The PVECs were treated with trypsin, and then immersed in 12 mL of cell culture media of the following composition. Some 4 % fetal bovine serum, 0.5 % penicillin/streptocillin, were added to 10 % RPMI medium 1640. Then, 25 μL of gentamin, and 20 μL of amphoterin B were added to 50 mL of the RPMI medium 1640 mixed with fetal bovine serum and penicillin/streptocillin.

PVECs Grown on PDMS

Plasma treated PDMS substrates were cut into 2.5 cm squares, and placed in 6-well culture plates. The 6-well plates and PDMS were placed in a sterilization bag, and treated with ethylene oxide (ETO). After the ETO treatment, the plates were degassed in a sterile hood for 24 hours. Then, some 2 mL the PVECs in cell culture media were added to the 6-well plates containing PDMS substrates. The experimenters adhered to strict sterile procedures at all times.

Force Measurements

Force measurements were done on a Digital Instruments Nanoscope III atomic force microscope. The experiment was conducted inside the fluid cell provided by the manufacturer. The fluid cell allows the solution to be exchanged without disturbing the experimental setup. A PDMS substrate grown with live PVECs was removed from the cell culture media and placed on an AFM substrate. The tip modified with SLe^X was placed in the tip holder, and measurements were taken directly on PVECs in phosphate buffered saline, pH 7.4. To calculate the adhesion force and the interaction energy, the radius of the particle was determined by optical microscopy and scanning electron microscopy. The spring constant, 0.12 N/m for the tip was obtained from the manufacturer (Digital Instruments, Santa Barbara, CA). To determine the nonspecific force of adhesion, force measurements were also performed in 7 M urea. Urea is a chaotropic agent that denatures proteins. Thus, the interactions measured would not involve specific binding between the sialyl Lewis X and the selectins.

Results and Discussion

The force curves showed two kinds of interactions. At small distances, there was a large interaction between the microsphere and the cell surface in both the test samples and the controls. At larger distances, there was a weaker interaction only between SLe^X and the selectins (Table 3.1). See Figure 3-3 for the force curves. Since there was no interaction between the controls (BSA on microspheres, no SLe^X), we hypothesized that the long-range interaction was the specific binding of SLe^X to P- and E- selectins on the surface of the cell.

Table 3-2. Data for interaction between glutaraldehyde reacted and sialyl Lewis X reacted microspheres and porcine vascular endothelial cells. The interaction between sialyl Lewis X and the endothelial cells showed two interactions.

Microsphere	Glutaraldehyde	SLe^X in 7M Urea	SLe^X-BSA, 1st interaction	SLe^X-BSA 2nd Interaction
Substrate	PVECs	PVECs	PVECs	PVECs
Distance (nm)	16.2 ± 2.9	21.3 ± 6.1	14.2 ± 3.1	106.7 ± 26.0
Force (nN/μm)	-0.27 ± 0.06	-0.28 ± 0.07	-0.21 ± 0.04	-0.46 ± 0.08

Using the Derjaguin approximation between a sphere of 5 μm radius and a flat surface, the short-range attractive interaction between SLe^X and ECs was calculated to be 0.21 ± 0.04 μN/μm (mean±standard deviation) at a distance of 14.2 ± 3.1 nm. The interaction between BSA and ECs was calculated to be 0.27±0.06 μN/μm at 16.2 ± 2.9 nm. After performing a t-test on the values of the attractive force, a p-value of 0.03355 was found. Thus, there is likely to be a significant difference between the strength of the interaction. A t-test was also performed on the distance of the force. In this case, a p-value 0.14999 was calculated. The difference in distances of the force may not be significant.

Between SLe^X and endothelial cells, a second interaction of 230.4±40.4 pN was measured at 106.7 ± 26.0 nm. There was no corresponding interaction on the control samples. Using the Derjaguin approximation, this value came to an interaction of 0.46±0.08 μN/μm. This force appeared to involve uncoiling of the selectin and rupture of the receptor-ligand bond. The mechanism for leukocyte rolling appears to involve the binding of the SLe^X to endothelial cells at short distances. Then the selectin acts as an uncoiling tether as the leukocyte rolls away from the endothelium. When the selectin is fully extended, the selectin-ligand bond ruptures. Figure 3-4 is a schematic of the leukocyte rolling process.

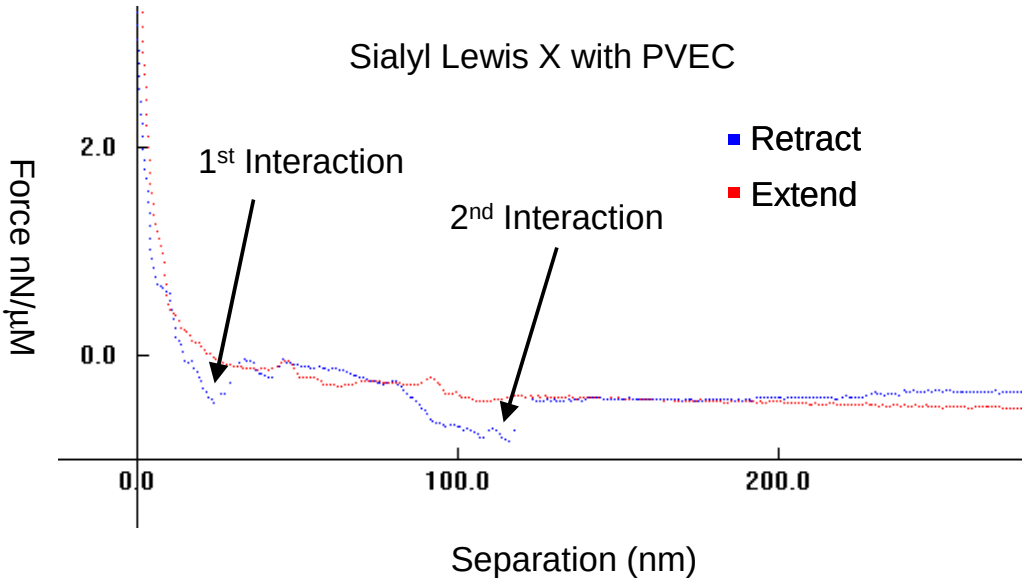

Figure 3-3. Sample force-separation curve showing both the initial nonspecific interaction and the second specific interaction.

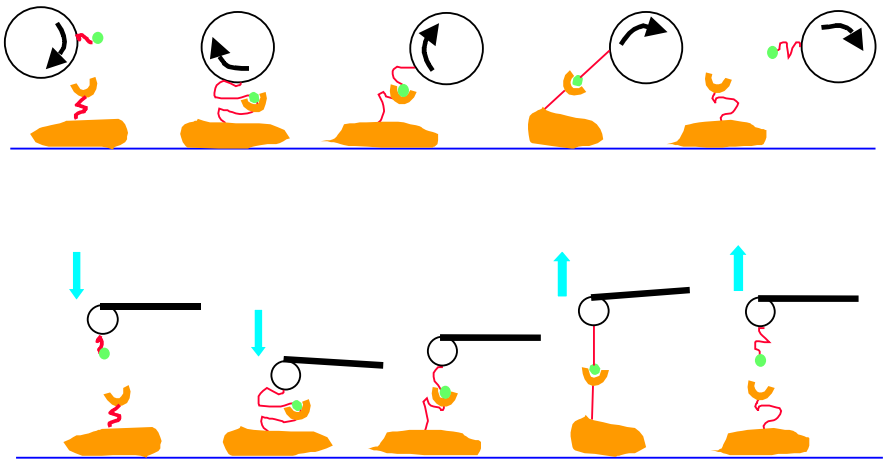

Figure 3-4. Schematic of how the leukocyte rolling process is simulated by the AFM.

When the SLe^X grafted microspheres were brought into contact with endothelial cells in 7M urea, there was only one interaction. The long-range interaction did not occur. At a distance of 21.3 ± 6.1 nm, there was an attractive interaction of 0.28 ± 0.07 nN/μm calculated using the Derjaguin approximation. A t-test was performed between the distance of the urea experiment and the first peak of the sialyl Lewis X experiment. A p-value of 8.89E-06 indicated that there was a significant difference in the distance of interaction. Between the forces of interaction in the urea experiment and the sialyl Lewis X experiment, $p = 0.067$. When the urea data and the force between the glutaraldehyde grafted microspheres and the ECs were compared, there were no significant differences in distance ($p = 0.556$) or strength of the force. Based on this data, one can conclude that the urea changed the binding between selectins and sialyl Lewis X because the forces and the distance of interaction between SLe^X grafted microspheres and ECs in PBS and in 7M urea are different. The forces and distance of interaction were not demonstrably different between SLe^X and ECs in urea, and glutaraldehyde grafted microspheres and ECs in PBS.

The denaturing effect of 7M urea may have altered the selectins such that the binding between SLe^X and the selectins was quantitatively similar to the nonspecific binding between glutaraldehyde grafted microspheres and ECs.

The interaction at distances greater than the distances for the second interaction between sialyl Lewis X grafted microspheres and ECs were also investigated. The slope of both the retraction and the extension curves between 200 nm and 700 nm were recorded (Table 3-3). The value of the force at 700 nm (in nN/μm) was subtracted from the value at 200 nm, and divided by 500 nm, resulting in a slope (in μN). All of the slopes were extremely close to zero, which indicates that at distances above 200 nm, the tip and the cell are not in contact. The lack of contact supports the explanation of selectin tethering given above. T-tests between the treatments indicate no significant differences ($P < 10E\text{-}4$ in all cases).

Table 3-3. Slope measured between 200 nm and 700 nm separation.

	Glutaraldehyde	SLe^X in 7M Urea	SLe^X-BSA
Slope of Retraction (μN)	-3.2E-5 ± 1.2E-3	7.0E-6 ± 6.3E-4	4.7E-6 ± 8.5E-4
Slope of Extension (μN)	-6.0E-5 ± 7.9E-4	-1.3E-5 ± 1.4E-3	-3.2E-5 ± 2.9E-4

These experiments demonstrate, for the first time by AFM, the fundamental forces involved in selectin-ligand interactions on cell surfaces. The long-range attraction between SLe^X and endothelial cells is indicative of SLe^X tethering by the selectin. This weak tethering slows down leukocytes as they roll, thus making selectins vital for leukocyte recruitment and diapedesis in the high shear stress vasculature. The short-range attraction is due to adhesion between the cell membrane and the microsphere. There are some differences between the strength of this short-range attraction for the test samples and the controls. The differences may be due to variables in the graft density of

BSA on the microsphere surface. The graft density may vary because the BSA-SLe^X would be less reactive, since the end modified with SLe^X would not react with the glutaraldehyde.

Future Work

This initial measurement of selectin-SLe^X interactions on the surface of cells leads to several intriguing possibilities in further basic research, and pharmaceutical and biomaterials development. First, the selectins may be further characterized and described in the terms and relationships of polymer physics. This will hasten the integration of physics, chemistry, and biology. This technique may be extended to other cell surface adhesion molecules. Integrins are the involved in the leukocyte adhesion process after selectin mediated rolling. The effects of hormones, cytokines, and other cellular signaling molecules on ligand-receptor binding can also be studied.

A better fundamental understanding of the selectins may lead to developments in pharmaceuticals and biomaterials. One possibility is the mapping of cell surfaces. The distribution of selectins, integrins, and antibodies on a cell surface may be mapped using their binding properties. Then the cell surface composition may be related to the effect of pharmaceuticals. The interactions between biomaterials and cells can also be studied using such a technique.

Structure/Property Relations of Individual Selectin Domains

An investigation into how each portion of the selectin molecule affects binding and rolling can be performed. As stated in the background, the exact composition of the

selectin differs among species and type (L-, E-, P-). A modification in the selectin composition, such as the reduction in the number of CB domains may change the distance of the interaction, and reduce the effectiveness of leukocyte rolling.

Investigation into Integrin Mediated Adhesion

After being slowed by rolling, integrins act to bind the leukocyte tightly to the endothelium surface prior to diapedesis. The forces of this interaction may be investigated in a similar fashion to the SLe^X-selectin experiment. The ligand for integrins is the repeat unit of the amino acids arginine, glycine, and aspartic acid, denoted by the abbreviation RGD.[126] The RGD tripeptide appears in fibronectin, vitronectin, osteopontin, collagen, thrombospondin, fibrinogen, and von Willebrand factor. This family of adhesion proteins and their integrin receptors act to provide cells with signals for polarity, differentiation, position, traction for migration, anchorage. An RGD containing molecule may be grafted to an AFM tip, and brought into contact with cells expressing integrins. The forces of interaction may be measured and compared with the selectin experiment outlined previously.

Cellular Environment and Pharmaceutical Effects

The interplay between leukocytes and endothelial cells involve two modes of communication. The first type, physical interaction mediated by receptor and counter-receptor molecules was investigated in this thesis, through the AFM investigation of selectin/sialyl Lewis X interaction. The second type occurs through the production of soluble mediators. These soluble polypeptide mediators are known as cytokines. These

molecules stimulate the expression of P- and E-selectins on endothelial cells. The addition of such signaling molecules may change the forces and distances of interaction, which can be characterized by the AFM. Similarly pharmaceuticals that affect the immune system also may be characterized by AFM.

Cell Surface Mapping

The increased interaction due to selectin-SLe^X binding can be used to create maps of cell surfaces. As the modified AFM tip is scanned across a cell, areas with selectins will be contrasted against areas lacking in selectins. Thus, the density of selectins on a cell surface may be measured. Recently, Hinterdorfer's group used molecular recognition of an antigen by an antibody to map a mica surface adsorbed with lysozymes.[40,127] The same type of recognition imaging may be used with selectins, and applied to studies of the surfaces of *ex vivo* vasculature. The density of selectin expression may be characterized as a function of blood flow and distance from injury.

CHAPTER 4

EFFECT OF TOPOGRAPHY ON CELL ADHESION

Background

The previous chapters of this thesis have focused on specific receptor-ligand interactions. To related the sub-micron scales of interaction investigated by the AFM to cellular level effects in the hierarchical system of cell adhesion, I also looked at the how topography affects cell adhesion. Specifically, I investigated how porcine vascular endothelial cells will adhere to micropatterned polydimethylsiloxane surfaces. It is known that cells display different behavior based on the topography of the surface. As mentioned earlier, many cells show anchorance dependence, meaning that cell growth and proliferation requires an adhesive surface. Thus, a better understanding of topographical effects is an important step in the creation of improved tissue scaffolding. Also, the physical effects of topography may be probed by the AFM. Although no study was performed in this thesis, which elements within the cell are affected by topography as evaluated by the AFM is a logical progression of this research. A review of the literature about topographical effects on cell adhesion is necessary to show what work has been done before.

Cell contacts often occur through a modality known as "focal adhesions." Focal adhesions involve integrins, which were introduced earlier as important mediators of the leukocyte rolling and adhesion process.[128] These integrins bind to adhesive proteins such

as fibronectin through an RGD sequence. Several intracellular proteins are also involved in binding, including talin, vinculin, and α-actinin. The α-actinin binds to actin microfilaments, causing alignment of the cell.[129] Since adhesive proteins such as fibronectin and vitronectin are present in most cell culture media, their adsorption onto biomaterial surfaces can significantly affect cell adhesion studies. Once the proteins have adsorbed to the biomaterial, cells adhere through integrin binding, and then begin to produce endogenous fibronectin to be deposited on the substrate. The deposition of fibronectin depends on the displacement of other proteins already adsorbed onto the substrate. The displacement is occurs more readily in hydrophilic substrates than hydrophobic substrates.[130,131] The relative ease of protein displacement does not necessarily explain whether hydrophilic or hydrophobic substrates will promote cell adhesion, however. The initial deposition of fibronectin may cause hydrophobic substrates to be conducive to cell adhesion.

To study the effect of topography on cell adhesion, a precise pattern of topography must be first generated. The most common method for producing patterns in PDMS is to first lithographically produce the pattern on a silicon wafer, and then replicate that pattern by casting onto the substrate. The type of lithography used is optimized for the size of the pattern. The smallest patterns are produced with direct write laser lithography and AFM lithography while those on the 2-10 μm scale are produced with UV photolithography.[132]

Patterns created on a substrate affects how cells bind and align, but the mechanism of this effect, referred with the encompassing term “contact guidance” have not been explained sufficiently. The width, the depth, the spacing between patterns, and

the preparation method all seem to have an effect.[132] Cell adhesion is also affected by the surface chemistry, the surface free energy and the kinetics of the binding.[132-134] Some general phenomena have been observed, however. First, groove widths in the sub-cellular range influences cell alignment in the direction of the grooves.[128,135] The depth of the groove has some influence, as deeper grooves allow bridging by the cell.[136] Surface features in the range of 1-5 μm seem to promote cellular conformation.

Schmidt and von Recum performed experiments with cell adhesion to patterned substrates.[133] Using microtextured silicone made by casting on a photoresist coated glass mask or silicon wafer. They varied the depth of the feature, and the spacing between different texture events. How murine peritoneal macrophages adhere to wells that ranged from smooth to 10 μm in width was studied. The arrays of these wells were arranged at variable distances from each other, causing an anisotropic pattern. The wells were also arranged a constant distance of 20.4 μm as an isotropic control. They found that some portion of the pattern must be anisotropic to invoke cell guidance. They also postulated that texture affects how cells adhere through both the surface area of adhesion and the perimeter of the area.

Contact guidance is also dependent on the type of cell or protein adhesion studied. In a later study by von Recum and others, patterns with groove widths of 2, 5, and 10 μm were coated with rat dermal fibroblasts.[134] The grooves were 0.5 μm deep, with ridges of the same width acting as separation. By measuring the alignment of the ECM protein deposited, the 2 μm pattern caused the most alignment, whereas the 5 and 10 μm patterns behaved more like a smooth surface. Variation of the chemical groups on a surface has also been studied. Britland *et al.* used photolithography to create a pattern of

aminosilane (AS) and a pattern of hydrophobic silane (HS) on glass slides.[137] The baby hamster kidney cells used in the study adhered preferentially on the aminosilane pattern. Cells also showed elongation along 10 μm AS tracks. One may view the AS pattern as a ligand that binds cells with greater affinity than the HS. Xiao and Truskey examined the ligand affinity issue.[138] This group also sees greater adhesion with increased ligand density, which they attribute to greater surface area. It is not a linear relationship. Using cyclic and linear compounds, they showed that similar compounds could have dramatically different affinities for the same receptor. This indicates that the combination of chemistry and topographical cues has a significant effect on cell adhesion. Besides the ligand affinity, ligand density also affects cell adhesion. As discussed in Chapter 1, Hammer's group was able to create a restricted mathematical model that solved how the ligand density affects the kinetics of cell detachment.[20]

Many of the studies done on patterned substrates have been conducted with PDMS. It provides an easily processed, low energy substrate that is well understood. Due to the low modulus, a precise reproduction of the pattern may be difficult to achieve, however. Thus, polystyrene, which allows improved precision of patterning, has been studied. Using polystyrene as the substrate, Walboomers *et al.* observed that the sharpness of the ridges was more important to contact guidance than the reduction of artifacts left behind from lithography.[139] The investigators also hypothesized that the contact guidance was caused by mechanical stress exerted by the topography.

Several groups focused on a patterned surface chemistry as a means of producing controlled cell growth on a surface. Potember, Matsuzawa, and Liesi grew dissociated embryonic rat hippocampal neurons on photolithigraphically patterned diethylenetriamine

(DETA) substrates.[14] A synthetic peptide, P1543 was used to make the surface bioactive, with plain DETA substrate as a control. Self-assembled monolayers prepared from n-octadecyltrichlorosilane (OTS) were used as a nonadhesive component. As a proof of nonadhesion, cells did not attach to the OTS substrates after 1.5 hours of incubation. The patterned DETA substrates were the poorest surfaces for neuron adhesion, producing clumps of short cells that did not mature, while the P1543 coated substrates promoted directional growth of 150-μm neurites.

Healy *et al.* used a completely chemical pattern on their substrate to examine the kinetics of organization and mineralization of rat calvaria bone cells.[141] The patterns were made by photolithographically producing a smooth surface of alternating surface chemistry. The pattern was alternating 50 μm strips of dimethyldichlorosilane (DMS) and N-(2-aminoethyl)-3-aminopropyl-trimethoxysilane (EDS). The experimenters concluded that the charge of the molecules on the surface was not the dominant mechanism for determining cell adhesion with bone cells. Rather, differences in cell adhesion were due to the adsorption of vitronectin onto the EDS regions, and the lack of adsorption in the DMS regions. The Healy group also evaluated the strength of cell adhesion through a probabilistic analysis.[142] Using a Weibull distribution, the investigators found a wide variation in the strength of adhesion in a cell population. This variation may be due to differences in the surface density of ligands, the density of receptor-ligand bonds, and the areas of focal contacts.

While most of the previous work described *in vitro* cell adhesion, a significant amount of *in vivo* work has also been performed. Since biomaterials often respond differently *in vivo*, a review of the literature is necessary to evaluate the differences. In an

attempt to promote the formation of a stable pseudo-neointima, patterns were made of Dacron polyester fibrils (250 μm long and 25 μm in diameter, variable spacing between fibrils) on polyurethane vascular patches. These patches were then implanted in sheep, along with a non-patterned control. One week after implantation, the entirety of the texture surface was covered by thrombus, while the non-textured surface was only partially covered. The authors hypothesized that the cause of the increase in thrombosis on the texture substrate was due to changes in flow conditions—the textured surface reduces local flow velocity.[128]

In another study, patterned silicone disks were implanted under the skin of New Zealand White rabbits.[143] The authors hypothesized that the microtexture would interlock with the fibrous capsule that typically forms around implants. This interlocking would limit movement of capsule, thus reducing mechanical irritation, and therefore, the capsule thickness. The thickness of the fibrous capsule did not vary significantly between the textured and smooth surfaces, however. The authors attributed this result to insufficiencies in the dimensions of the grooves and ridges. SEM showed that fibroblasts did not orient parallel to the grooves *in vivo*, which contradicts previous *in vitro* studies.[144] Since the work related in my thesis is an *in vitro* study, some of the trends observed here may be expected to differ *in vivo*.

Walboomer and colleagues have extensively studied contact guidance both *in vitro* and *in vivo*, and may give some insights into how the two environments affects cell adhesion. In one study, rat dermal fibroblasts were cultured on polystyrene (PS), titanium coated polystyrene (PSTi), silicone (SIL), and poly-L-lactic acid (PLL) of depths of 0.5 μm, and groove widths between 1 and 10 μm.[145] Treatment with radiofrequency glow

discharge plasma (RF plasma) to increase the hydrophilicity was another variable. The common topography between the surfaces indicates that differences in proliferation and orientation may be attributed to surface chemistry effects. The RF plasma treatment increased cell proliferation. For the untreated samples, PLL and SIL showed the most proliferation, with less for PS and PSTi. Cell alignment seems dependent on both the groove width and the surface chemistry. So for PS and SIL, cells did not align on 10 μm wide grooves, but did on 1 μm grooves. No such correlation with groove width was observed with PSTi, however. Cells aligned regardless of the width. The fibroblasts were most strongly aligned on the PLL, and increase in alignment correlated with decreasing groove width. In another study, Walboomers *et al.* examined the effect of depth (0.5, 1.0, 1.8, and 5.4 μm) and width (1, 2, 5, 10, and 20 μm) of fibroblast alignment on polystyrene.[146] The cell orientation seems to increase with groove depth: 1.8 and 5.4 μm showed the most alignment. Fibroblasts exhibited bridging of the deeper grooves, which the authors attributed to high membrane stiffness that do not allow the cell to bend into the deep grooves. Contrary to previous observations on PS,[145] the groove width did not correlate to significant differences in cell alignment. For *in vivo* studies, Walboomer *et al.* implanted microtextured PS in goats[147] and microtextured silicone in guinea pigs.[148] The increased complexity of the animal model leads to different observations *in vivo* and *in vitro*. *In vivo*, the interplay of several cell types leads to the formation of a fibrous capsule around the textured implant. In both studies, showed no significant differences in morphology of the capsules around textured and smooth implants.

In summary, the previous work mainly involved phenomenological observations of how and whether cells proliferated and aligned to various substrates. The exact cellular mechanisms of contact guidance have not been elucidated. The staining methods outlined in this chapter are a first step toward determining which portion of the cell is affected by topography. Furthermore, the techniques involving AFM force measurements related in Chapters 2 and 3 may be applied to this study. The changes in the expression of cell adhesion molecules due to topography may be monitored by AFM.

Materials and Methods

We grew porcine vascular endothelial cells on polydimethyl siloxane substrates (PDMS). The PDMS substrates were cast on polystyrene templates made through replication of microtextured silicon wafers. Other members of the Brennan research group generously provided the polystyrene templates and the microtextured silicon wafers, so the details of their manufacture will not be divulged here. After treatment with RF plasma, substrates were sterilized. Cells were obtained from Dr. Edward Block's group at the Malcom Randall Veterans Adminstration medical center, and grown using standard cell culture techniques. The cell morphology on PDMS substrates was observed through optical microscopy, scanning electron microscopy, and scanning laser confocal microscopy.

Synthesis of PDMS

T-2 Silastic silicone elastomer resin and base were obtained from Dow Corning. The exact composition of the T-2 Silastic is proprietary, but the basic components of

vinyl functionalized PDMS, and a platinum crosslinking agent are present. The base and the resin are mixed together in a 10:1 ratio, degassed in a vacuum, and cast on patterned silicon substrates for 24 hours. In this study the depth of the topography was a constant 5 μm. Groove width was varied between 5, 10, and 20 μm. Nobs were also made with separations of 5, 10, and 20 μm.

Porcine Vascular Endothelial Cell (PVEC) Culture

PVECs were obtained from Dr. Edward Block's group. The PVECs were treated with trypsin, and then immersed in 12 mL of cell culture media of the following composition. Some 4 % fetal bovine serum, 0.5 % penicillin/streptocillin, was added to 10 % RPMI medium 1640. Then, 25 μL of gentamin, and 20 μL of amphoterin B were added to 50 mL of the RPMI medium 1640 mixed with fetal bovine serum and penicillin/streptocillin.

Plasma Treatment of PDMS Substrates

Some of the PDMS substrates were treated by radio frequency glow discharge plasma to improve cell adhesion by creating hydrophilic groups on the hydrophobic PDMS. Using a RF Plasma Inc. HFS 401S instrument, set at 50 watts, the PDMS samples were plasma treated at 40 mTorr of vacuum in Argon for 5 minutes.

Fibronectin Coating of PDMS Substrates

Another method to improve cell adhesion was by coating the PDMS substrate with fibronectin. After sterilization, the substrates were soaked in a 4 μg/mL solution of

fibronectin (Sigma-Aldrich, St. Louis, MO) for two hours. Then, the solution was siphoned off, and endothelial cells were added immediately.

PVECs Grown on PDMS

Plasma treated PDMS substrates were cut into 2.5 cm squares, and placed in 6-well culture plates. The 6-well plates and PDMS were placed in a sterilization bag, and treated with ethylene oxide (ETO). After the ETO treatment, the plates were degassed in a sterile hood for 24 hours. Then, some 2mL the PVECs in cell culture media were added to the 6-well plates containing PDMS substrates. The experimenter adhered to strict sterile procedures at all times. Observations were made after three days of growth. The cell culture media was changed every other day.

Optical Microscopy

The cells grown on PDMS were placed under an optical microscope, and viewed at 10X. The cells were not stained. Pictures were taken with a digital camera.

Scanning Electron Microscopy

The experimenters used a JEOL 6400 scanning electron microscope to view the microtextured substrates. After fixing the cells with Trump's solution (glutaraldehyde and formaldehyde), the samples were washed with phosphate buffered saline, pH = 7.4. Then, a sequential wash was performed using DI water and 100 % ethanol in 20 vol% increments. For example, initially, the sample was washed with 100 % DI water. Then, the sample was washed with 20 vol% ethanol in DI water. The ethanol was gradually

increased to 100 % ethanol. The samples were allowed to dry in air, and mounted on SEM sample holders with carbon glue. The samples were then coated with gold and palladium.

Scanning Laser Confocal Microscopy

Two methods of staining were used. First, von Willebrand factor, a blood glycoprotein required for platelet adhesion that is made by endothelial cells, was stained. The endothelial cells grown on PDMS were washed twice with phosphate buffered saline (PBS), and fixed with acetone at –20 °C for 15 minutes. After another two washes in PBS, the substrates were placed in a 0.46 μg/mL solution of goat anti-human von Willebrand factor biotinylated IgG for 1 hour. The sample was then washed in PBS twice, and placed in 5 μg/mL solution of streptavidin-fluorescein for 1 hour. After another wash with PBS, the sample was inverted onto a glass coverslip. Silicone vacuum grease was placed on the outer edges of the sample to create some separation between the sample and the glass, so as to not crush the cells and deform the patterns.

The second method used fluorescein labeled GSL-1 isolectin B4 (Burlingame, CA) to stain carbohydrates on the cell membrane. After washing with PBS, fixing wit acetone, and a second wash with PBS (same details as above), the fixed endothelial cells on PDMS were placed in a 10 μg/mL solution of the GSL-1 isolectin B4. Since the isolectin was already labeled with fluorescein, no further staining was necessary. The sample was washed, and placed on a glass coverslip with the same methods reported in the previous paragraph. Images were taken with a Zeiss LSM 430 scanning laser confocal microscope.

Results and Discussion

Porcine vascular endothelial cells adhered minimally to plain PDMS substrates (Fig 4.1). When the substrate was treated with fibronectin, cell adhesion was improved (Fig 4.2). Scanning electron microscopy showed that addition of fibronectin obscured the topography, however (Fig 4.3). Thus, RF plasma was used to modify the surface. The RF plasma treated surface improved cell adhesion (Fig 4.4). The morphology of the cells on the PDMS substrate was investigated using the SEM. Some cells appear to pull the ridges toward themselves (Fig 4.5). When the PDMS substrate is viewed along the topography, some cells appear to be bridging the groove (Fig 4.6). Cells observed under the scanning laser confocal microscope show deformation of the ridges (Fig 4.7), but the resolution was not high enough to observe bridging. Walboomers *et al.* previously observed similar deformation of silicone substrates with rat dermal fibroblasts.[145]

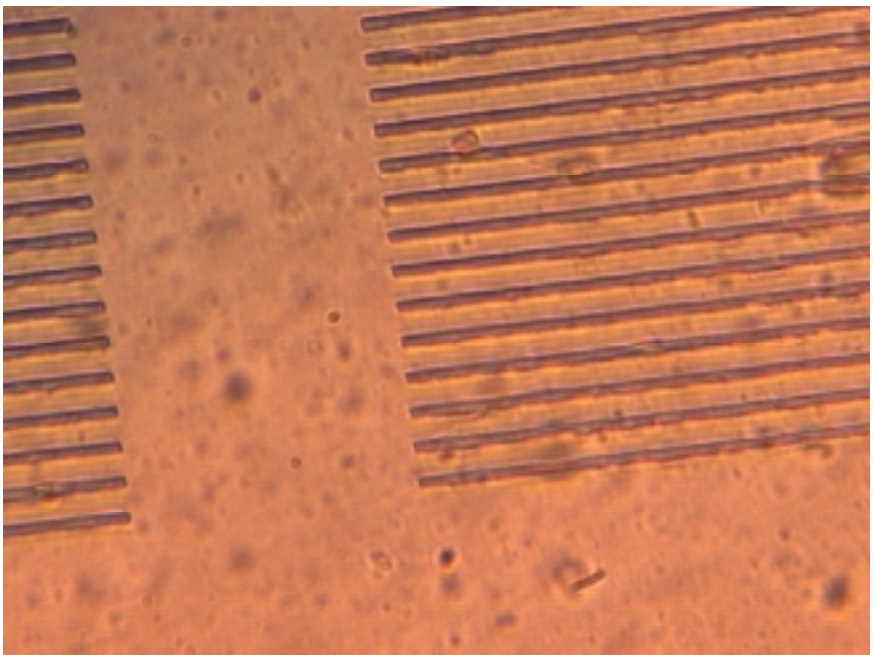

Figure 4-1. Plain PDMS. Efforts at growing endothelial cells the surface did not lead to a confluent layer. There are very few cells on the surface. The ridges are separated by 10 μm.

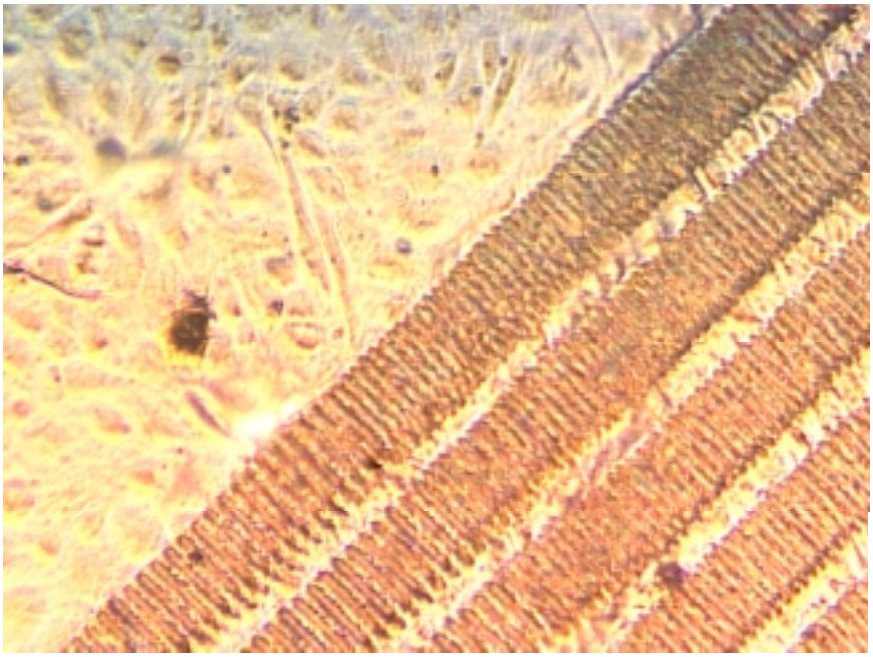

Figure 4-2. Endothelial cells grown on textured substrate coated with fibronectin. The separation between the on the upper right is 5 μm, and between the ridges on the lower left is 10 μm.

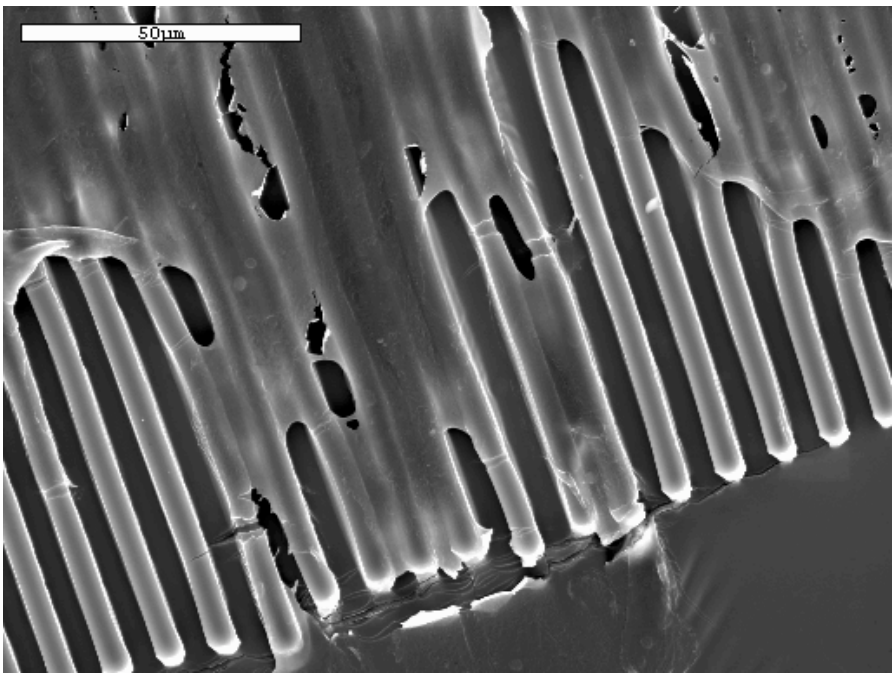

Figure 4-3. SEM of PDMS substrate coated with fibronectin. The fibronectin seem to obscure the features, and deform the ridges.

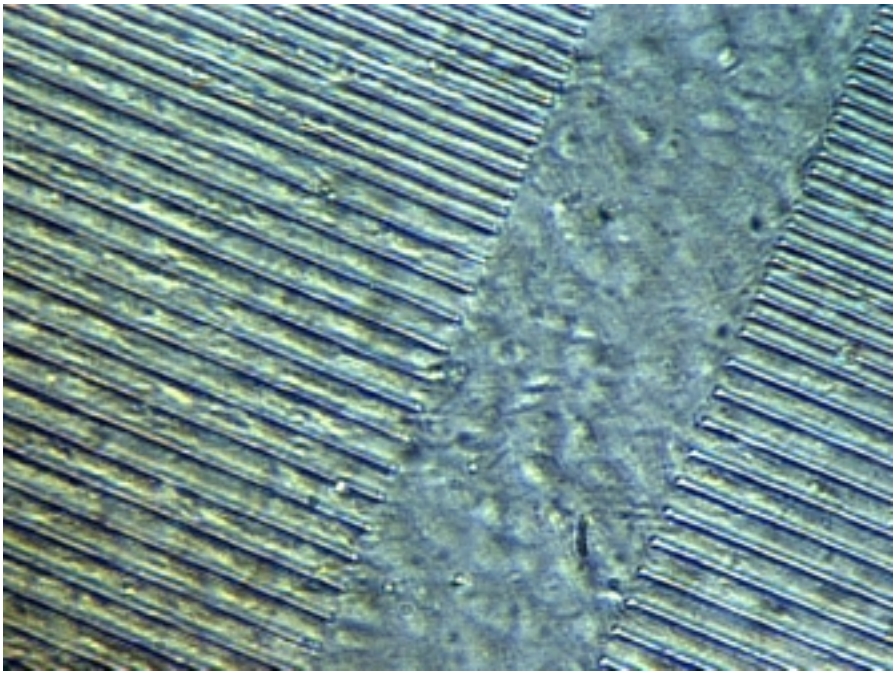

Figure 4-4. Optical microscopy picture of PDMS substrate treated with RF plasma. Notice the confluent cell layer in the middle region with no topography. The separation between ridges on the upper right is 5 µm, and on the lower left is 10 µm.

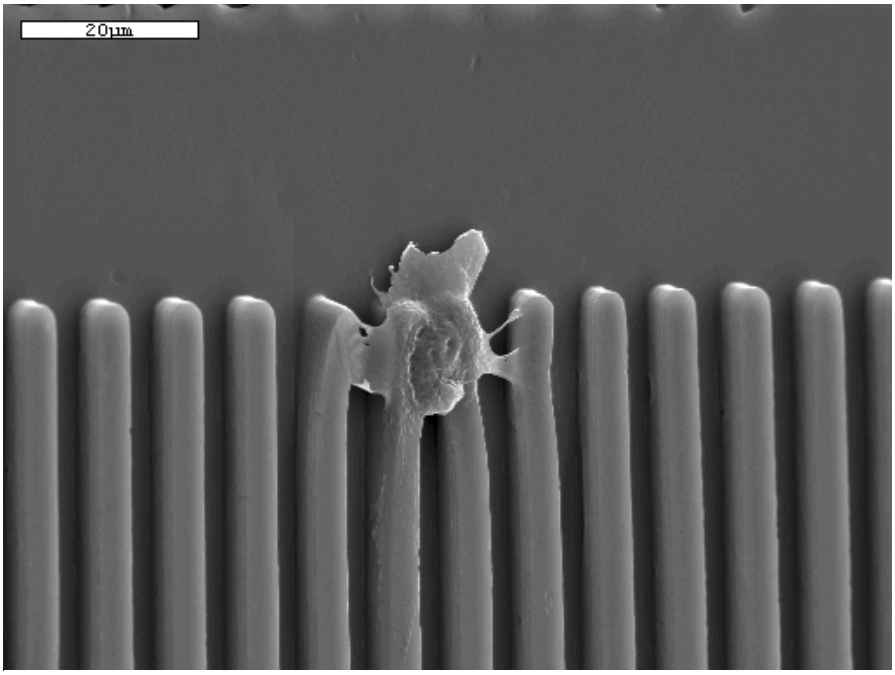

Figure 4-5. SEM of a cell deflecting the ridges of the PDMS substrate.

Figure 4-6. SEM of 5µm high ridges. A cell appears to be bridging the 10µm groove between the ridges.

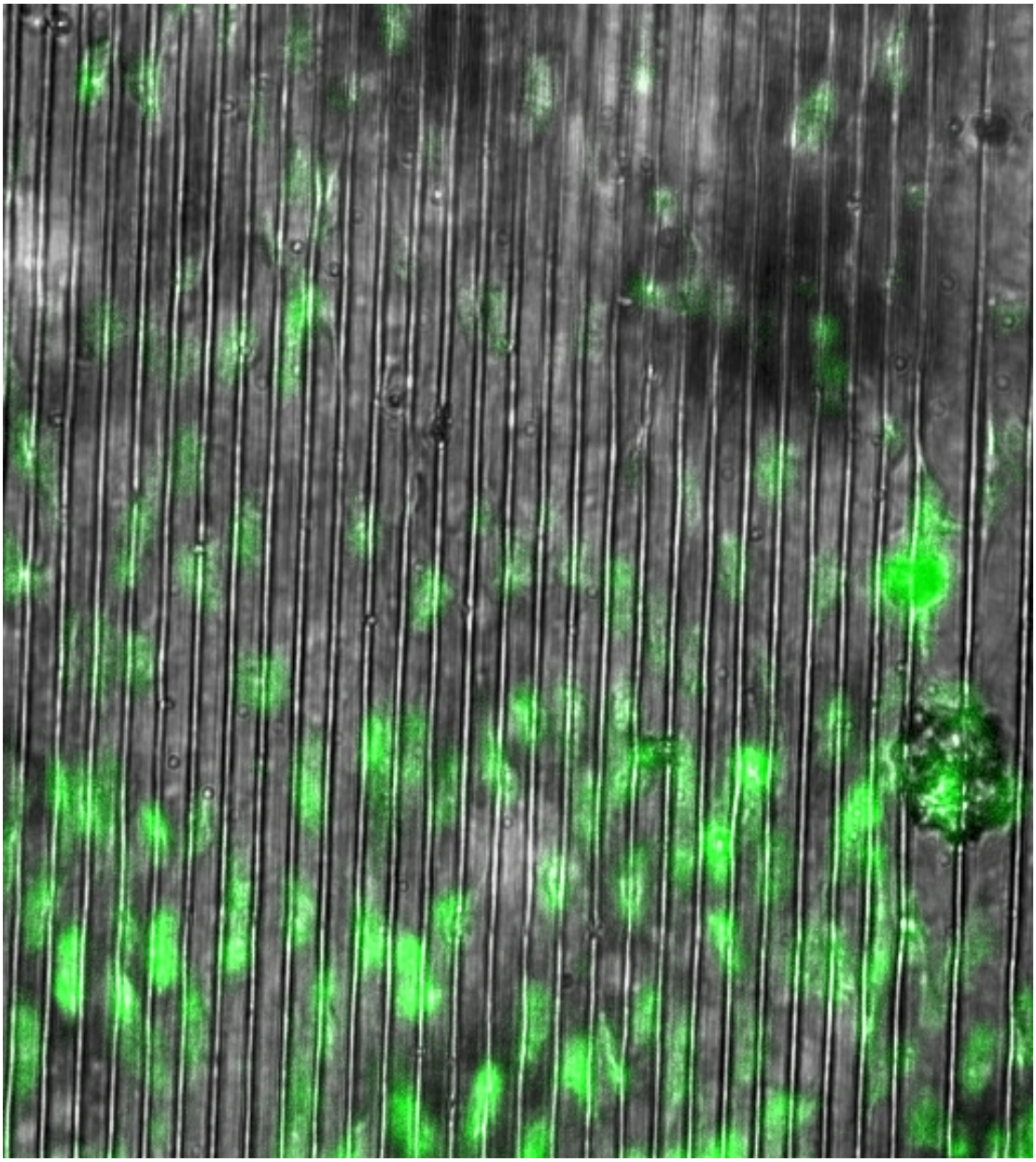

Figure 4-7. Scanning laser confocal microscopy image of endothelial cells stained with goat anti-human von Willebrand factor biotinylated IgG on PDMS substrates. The sample is at a small tilt, which means that the focal plane only captures a few cells (indicated by the green coloring). Thus, cells are not present in greater quantities on the bottom of the sample. Notice that the cells appear to distort the PDMS ridges.

This thrust of my thesis is inchoate. The methodologies of observing cell adhesion (i.e. cell staining for laser confocal microscopy, sample preparation for SEM) were developed, but deficiencies in time precluded a systematic study. Several issues remain unresolved. The preparation of samples for SEM requires desiccation of the cells, which may create artifacts. The staining intensity and resolution of the laser confocal microscope must be improved to allow the creation of meaning three-dimensional projections from pictures taken at a various focal planes.

Future Work

Endothelial cell adhesion on the microtextured PDMS substrates, as characterized through laser confocal microscopy, will be correlated to the width of ridges, the width of the valleys, and the height of the ridges. The topography for maximal and minimal cell adhesion may be determined. Other types of cells may be introduced to the system. Smooth muscle cells may be used in conjunction with endothelial cells to determine if the interplay of the two cell types creates variations in contact guidance. Since the ultimate goal of this study is improved biomaterials for clinical applications, a study of the behavior microtextured devices *in vivo* is necessary. The patterned surfaces will be converted to a device, and implanted into an animal model.

CHAPTER 5

CONCLUSION

In my thesis I investigated two aspects of cell adhesion. At the molecular level, specific receptor-ligand interactions were probed. In the avidin-biotin system, I observed a significant increase in the force of adhesion, which indicates that avidin grafted onto glass substrates bound specifically to biotin. I also showed that the addition of free biotin to the environment in which the force measurements were taken did not alter the force of adhesion specifically. In the selectin-sialyl Lewis X system, I observed interactions at two distances. First, a nonspecific interaction attributed to the adhesion of the microsphere to the cell membrane occurred at close range. At longer distances, a second interaction occurred. Based on the model of leukocyte rolling, the second interaction indicates elastic tethering of the sialyl Lewis X by the selectin. This is the first measurement of the adhesive forces of selectins on endothelial cells by atomic force microscopy.

At the cellular level, I investigated the effect of topography on endothelial cell proliferation and orientation. Porcine vascular endothelial cells were grown on PDMS substrates. The proliferation of the cells was improved when the substrate was coated with fibronectin or made more hydrophilic with RF plasma. The cells appear to deform the ridges on the PDMS, and possibly bridge the groove between ridges.

More work is required in both of these topics. By measuring the adhesive forces with the AFM, an investigator may determine both the density and the affinity of expressed of cell adhesion molecules. This may lead to a better understanding of how topography affects cell adhesion. The surface densities of selectins or other cell adhesion molecules may correlate with differences in the topography of the substrate. While the two aspects of cell adhesion covered in my thesis may seem dissimilar—they occur at different levels of complexity, with further work in the molecular level, the mechanisms behind contact guidance may be elucidated.

LIST OF REFERENCES

1. Rubin, G.M., Yandell, M.D., Wortman, J.R., Gabor Miklos, G.L., Nelson, C.R., Hariharan, I.K., Fortini, M.E., Li, P.W., Apweiler, R., Fleischmann, W., Cherry, J.M., Henikoff, S., Skupski, M.P., Misra, S., Ashburner, M., Birney, E., Boguski M.S., Brody, T., Brokstein, P., Celniker, S.E., Chervitz, S.A., Coates, D., Cravchik, A., Gabrielian, A., Galle, R.F., Gelbart, W.M., George, R.A., Goldstein, L.S., Gong, F., Guan, P., Harris, N.L., Hay, B.A., Hoskins, R.A., Li, J., Li, Z., Hynes, R.O., Jones, S.J., Kuehl, P.M., Lemaitre, B., Littleton, J.T., Morrison, D.K., Mungall, C., O'Farrell, P.H., Pickeral, O.K., Shue, C., Vosshall, L.B., Zhang, J., Zhao, Q., Zheng, X.H., Zhong, F., Zhong, W., Gibbs, R., Venter, J.C., Adams, M.D. & Lewis, S. (2000) Science 287, 2204-15.

2. Chervitz, S., Aravind, L., Sherlock, G., Ball, C.A., Koonin, E.V., Dwight, S.S., Harris, M.A., Dolinski, K., Mohr, S., Smith, T., Weng, S., Cherry, J.M. & Botstein, D. (1998) Science 282, 2022-8.

3. Moore, W. S. (1993) (W. B. Saunders Company, Philadelphia), pp. 870.

4. Bevilacqua, M. P., Nelson, R. M., Mannori, G. & Cecconic, O. (1994) Annu Rev Med 45, 361-378.

5. Bevilacqua, M. P. & Nelson, R. M. (1993) J Clin Invest 91, 379-387.

6. Travis, J. (1993) Science 40, 906-908.

7. Tanabe, K. K. & Saya, H. (1994) Crit Rev Oncog 5, 201-12.

8. Greisler, H. P. (1991) Xanthus Intelligence Unit Report No. 3 (R. G. Landes Company, Austin, TX).

9. Schneider, A., Melmed, R. N., Schwalb, H., Karck, M., Vlodavsky, I. & Uretzky, G. (1992) J Vasc Surg 15, 649-656.

10. Magometschnigg, H., Kadletz, M., Vodrazka, M., Dock, W., Grimm, M., Grabenwoger, M., Minar, E., Staudacher, M., Fenzl, G. & Wolner, E. (1992) J Vasc Surg 15, 527-35.

11. Cenni, E., Arciola, C. R., Ciapetti, G., Granchi, D., Savarino, L., Stea, S., Cavedagna, D., Curti, T., Falsone, G. & Pizzoferrato, A. (1995) Biomaterials 16, 973-976.

12. Sbarbati, R., Giannessi, D., Cenni, M. C., Lazzerini, G., Verni, F. & Caterina, R. D. (1991) Biomaterials 14, 491-498.

13. Paulsson, M., Gouda, I., Larm, O. & Ljungh, A. (1994) J Biomed Mater Res 28, 311-317.

14. Phaneuf, M. D., Berceli, S. A., Bide, M. J., Quist, W. C. & LoGerfo, F. W. (1997) Biomaterials 18, 755-765.

15. Nicol, A., Gowda, D. C. & Urry, D. W. (1992) J Biomed Mater Res 26, 393-413.

16. Ito, Y., Kajihara, M. & Imanishi, Y. (1991) J Biomed Mater Res 25, 1325-1337.

17. Cozens-Roberts, C., Lauffenburger, D. A. & Quinn, J. A. (1990) Biophys J 58, 841-856.

18. Cozens-Roberts, C., Quinn, J. A. & Lauffenburger, D. A. (1990) Biophys J. 58, 107-125.

19. Bell, G. I. (1978) Science 200, 618-627.

20. Ward, M. D., Dembo, M. & Hammer, D. A. (1995) Ann Biomed Eng 23, 322-331.

21. Hammer, D. A. & Apte, S. M. (1992) Biophys. J. 63, 35-57.

22. Israelachvili, J. N. & Adams, G. E. (1978) J Chem Soc Faraday Trans. 1 74, 975.

23. Binnig, G., Rohrer, H., Gerber, C. & Weibel, E. (1982) Phys Rev Lett 49, 57-61.

24. Binnig, G., Quate, C. F. & Gerber, C. (1986) Phys Rev Lett 56, 930-933.

25. Suzuki, A., Yamazaki, M., Kobiki, Y. & Suzuki, H. (1997) Macromolecules 30, 2350-2354.

26. Suzuki, A., Yamazaki, M. & Kobiki, Y. (1995) J Chem Phys 104, 1751-1757.

27. Craig, V. S. J., Hyde, A. M. & Pashley, R. M. (1996) Langmuir 12, 3557-3562.

28. Ducker, W. A., Senden, T. J. & Pashley, R. M. (1991) Nature 353, 239-241.

29. Ducker, W. A., Senden, T. J. & Pashley, R. M. (1992) Langmuir 8, 1831-1836.

30. Meagher, L. & Pashley, R. M. (1995) Langmuir 11, 4019-4024.

31. Karaman, M. E., Meagher, L. & Pashley, R. M. (1993) Langmuir 9, 1220-1227.

32. Meagher, L. & Craig, V. S. J. (1994) Langmuir 10, 2736.

33. Larson, I., Drummond, C. J. & Chan, D. Y. C. (1993) J Am Chem Soc 115, 25.

34. Biggs, S., Chow, M. K., Zukoski, C. F. & Grieser, F. (1993) J Colloid Interface Sci 160, 511.

35. Sagvolden, G., Giaever, I., Pettersen, E. O. & Feder, J. (1999) Proc Natl Acad Sci USA 96, 471-476.

36. Holland, N. B., Siedlecki, C. A. & Marchant, R. E. (1999) J Biomed Mater Res 45, 167-174.

37. Florin, E., Moy, V. & Gaub, H. (1994) Science 264, 415.

38. Moy, V., Florin, E. & Gaub, H. (1994) Coll Surf A 93, 343.

39. Ludwig, M., Moy, V., Rief, M., Florin, E. & Gaub, H. (1994) Microsc Microanal Microstruct 5, 321.

40. Raab, A., Han, W., Badt, D., Smith-Gill, S. J., Lindsay, S. M., Schindler, H. & Hinterdorfer, P. (1999) Nat Biotechnol 17, 902-905.

41. Ducker, W. A., Xu, Z. & Israelachvili, J. N. (1994) Langmuir 10, 3279-3289.

42. Israelachvili, J. N., Tirrell, M., Klein, J. & Almog, Y. a. (1984) Macromolecules 17, 204-209.

43. Israelachvili, J. N. & Wennerstrom, H. (1996) Nature 379, 219-225.

44. Kamiyama, Y. & Israelachvili, J. (1992) Macromolecules 25, 5081-5088.

45. Klein, J., Kamiyama, Y., Yoshizawa, H., Israelachvili, J. N., Fetters, L. J. & Pincus, P. (1992) Macromolecules 25, 2062-2064.

46. Klein, J., Kamiyama, Y., Yoshizawa, H., Israelachvili, J. N., Fredrickson, G. H., Pincus, P. & Fetters, L. J. (1993) Macromolecules 26, 5552-5560.

47. Ruths, M., Yoshizawa, H., Fetters, L. J. & Israelachvili, J. N. (1996) Macromolecules 29, 7193-7203.

48. Wong, J. Y., Kuhl, T. L., Israelachvili, J. N., Mullah, N. & Zalipsky, S. (1997) Science 275, 820-822.

49. Klein, J. & Luckham, P. (1982) Nature 300, 429-431.

50. Klein, J. (1983) J Chem Soc Faraday Trans I 79, 99-118.

51. Klein, J. & Luckham, P. F. (1984) Macromolecules 17, 1041-1048.

52. Klein, J., Kumacheva, E., Mahalu, D., Perahia, D. & Fetters, L. J. (1994) Nature 370, 634-636.

53. Kumacheva, E., Klein, J., Pincus, P. & Fetters, L. J. (1993) Macromolecules 26, 6477-6482.

54. Luckham, P. F. & Klein, J. (1985) Macromolecules 18, 721-728.

55. Luckham, P. & Klein, J. (1990) J Chem Soc Faraday Trans I 86, 1363-1368.

56. Taunton, H. J., Toprakcioglu, C., Fetters, L. J. & Klein, J. (1990) Macromolecules 23, 571-580.

57. Briscoe, B., Luckham, P. & Zhu, S. (1996) Macromolecules 29, 6208-6211.

58. Claesson, P. (1993) Colloids Surf A: Phys Eng Aspects 77, 109-118.

59. Claesson, P. M., Ederth, T., Bergeron, V. & Rutland, M. W. (1996) Adv Colloid Interface Sci 67, 119-183.

60. Claesson, P. M., Blomberg, E., Paulson, O. & Malmsten, M. (1996) Colloids Surf A: Phys Eng Aspects 112, 131-139.

61. Malmsten, M., Claesson, P. M., Pezron, E. & Pezron, I. (1990) Langmuir 6, 1572-1578.

62. Malmsten, M. & Claesson, P. M. (1991) Langmuir 7, 988-994.

63. Green, N. M. (1975) Adv Protein Chem 29, 85-133.

64. Florin, E.-L., Moy, V. T. & Gaub, H. E. (1994) Science 264, 415-417.

65. Moy, V. T., Florin, E.-L. & Gaub, H. E. (1994) Science 266, 257-259.

66. Weber, P. C., Ohlendorf, D. H., Wendoloski, J. J. & Salemme, F. R. (1989) Science 243, 85-88.

67. Hendrickson, W. A., Pahler, A., Smith, J. L., Satow, Y., Merrit, E. A. & Phizackerley, R. P. (1989) Proc Natl Acad Sci USA 86, 2190-2194.

68. Weber, P. C., Pantoliano, M. W. & Salemme, F. R. (1995) Acta Crystalllogr D 51, 590-596.

69. Jones, M. L. & Kurzban, G. P. (1995) Biochemistry 34, 11750-11756.

70. Livnah, O., Bayer, E. A., Wilchek, M. & Sussman, J. L. (1993) Proc Natl Acad Sci USA 90, 5076-5080.

71. Chilkoti, A. & Stayton, P. S. (1995) J Am Chem Soc 117, 10622-10628.

72. Pugliese, L., Coda, A., Malcovati, M. & Bolognesi, M. (1993) J Mol Biol 231, 698-710.

73. Weber, P. C., Wendoloski, J. J., Pantoliano, M. W. & Salemme, F. R. (1992) J Am Chem Soc 114, 3197-3200.

74. Miyamoto, S. & Kollman, P. A. (1993) Proteins 16, 226-245.

75. Chilkoti, A., Boland, T., Ratner, B. D. & Stayton, P. S. (1995) Biophys J 69, 2125-2130.

76. Grubmuller, H., Heymann, B. & Tavan, P. (1996) Science 271, 997-999.

77. Tedder, T. F., Steeber, D. A., Chen, A. & Engel, P. (1995) FASEB J 9, 866-873.

78. Etzioni, A., Phillips, L. M., Paulson, J. C. & Harlan, J. M. (1995) Ciba Found Symp 189, 51.

79. Seekamp, A., Till, G. O., Mulligan, M. S., Paulson, J. C., Anderson, D. C., Miyasaka, M. & Ward, P. A. (1994) Am J Pathol 144, 592-598.

80. Subramaniam, M., Saffaripour, S., Van De Water, L. V. D., Frenette, P. S., Mayadas, T. N., Hynes, R. O. & Wagner, D. D. (1997) Am J Pathol 150, 1701-1709.

81. Santos-Benito, F. F., Fernandez-Meyorales, A. & Martin-Lornas, M. (1992) J Exp Med 176, 915-918.

82. Baggiolini, M., Dewald, B. & Moser, B. (1997) Annu Rev Immunol 15, 675-705.

83. Zimmerman, G. A., McIntyre, T. M. & Prescott, S. M. (1996) J Clin Invest 98, 1699-1701.

84. Drickamer, K. (1988) J Biol Chem 268, 9557-9560.

85. Patel, K. D., Nollert, M. U. & McEver, R. P. (1995) J Cell Biol 131, 1893-1902.

86. Vestweber, D. & Blanks, J. E. (1999) Physiol Rev 79, 181-213.

87. Bevilacqua, M. P., Pober, J. S., Mendrick, D. L., Cotran, R. S. & Jr, M. A. G. (1987) Proc Natl Acad Sci USA 84, 9238-9242.

88. Pober, J. S., Lapierre, L. A., Stolpen, A. H., Brock, T. A., Springer, A. T., Fiers, W., Bevilacqua, M. P., Mendrick, D. L. & Jr, M. A. G. (1987) J Immunol 138, 3319-3324.

89. Geng, J.-G., Bevilacqua, M. P., Moore, K. L., McIntyre, T. M., Prescott, S. M., Kim, J. M., Bliss, G. A., Zimmerman, G. A. & McEver, R. P. (1990) Nature 343, 757-760.

90. Dembo, M., Torney, D. C., Saxman, K. & Hammer, D. (1988) Proc R Soc Lond B Biol Sci 234, 55-83.

91. Hammer, D. A. & Apte, S. M. (1992) Biophys J 63, 35-57.

92. Lawrence, M. B. & Springer, T. A. (1991) Cell 65.

93. Brandley, B. K., Kiso, M., Abbas, S., Nikrad, P., Srivasatava, O., Foxall, C., Oda, Y. & Hasegawa, A. (1993) Glycobiology 3, 633-641.

94. Cooke, R. M., Hale, R. S., Lister, S. G., Shah, G. & Weir, M. P. (1994) Biochemistry 33, 10591-10596.

95. Foxalll, C., Watson, S. R., Dowbenko, D., Fennie, C., Lasky, L. A., Kiso, M., Hasegawa, A., Asa, D. & Brandley, B. K. (1992) J Cell Biol 117, 895-902.

96. Jacob, G. S., Kirmaier, C., Abbas, S. Z., Howard, S. C., Steininger, C. N., Welply, J. K. & Scudder, P. (1995) Biochemistry 34, 1210-1217.

97. Nelson, R. M., Dolich, S., Aruffo, A., Cecconi, O. & Bevilacqua, M. P. (1993) J Clin Invest 91, 1157-1166.

98. Sanders, W. J., Katsumoto, T. R., Bertozzi, C. R., Rosen, S. D. & Kiessling, L. L. (1996) Biochemistry 35, 14862-14867.

99. Nicholson, M. W., Barclay, A. N., Singer, M. S., Rosen, S. D. & Merwe, A. V. D. (1998) J Biol Chem 273, 749-755.

100. Mehta, P., Cummings, R. D. & McEver, R. P. (1998) J Cell Biochem S24A, X5-210.

101. Alon, R., Hammer, D. A. & Springer, T. A. (1995) Nature 374, 539-542.

102. Alon, R., Chen, S., Puri, K. D., Finger, E. B. & Springer, T. A. (1997) J Cell Biol 138, 1169-1180.

103. Jung, U., Bullard, D. C., Tedder, T. F. & Ley, K. (1996) Am J Physiol 271, H2740-H2747.

104. Kunkel, E. J. & Ley, K. (1996) Circ Res 79, 1196-1204.

105. Puri, K. D., Finger, E. B. & Springer, T. A. (1997) J Immunol 158, 405-413.

106. Clark, R. A., erickson, H. P. & Springer, T. A. (1997) J Cell Biol 137, 755-765.

107. Berlin, C., Bargatze, R. F., Campbell, J. J., Andrian, U. H. V., Szabo, M. C., Hasslen, S. R., Nelson, R. D., Berg, E. L., Erlandsen, S. L. & Butcher, E. C. (1995) Cell 80, 413-422.

108. Clark, R. A., Alon, R. & Springer, T. A. (1996) J Cell Biol 134, 1075-1087.

109. Dengrendele, H. C., Estess, P., Picker, L. J. & Siegelman, M. H. (1996) J Exp Med 183, 1119-1130.

110. Chen, S., Alon, R., Fuhlbrigge, R. C. & Springer, T. A. (1997) Pro Natl Acad Sci USA 94, 3172-3177.

111. Finger, E. B., Puri, K. D., Alon, R., Lawrence, M. B., Andrian, U. H. V. & Springer, T. A. (1996) Nature 379, 266-269.

112. Lawrence, M. B., Kansas, G. S., Kunkel, E. J. & Ley, K. (1997) J Cell Biol 136, 717-727.

113. Taylor, A. D., Neelamegham, S., Hellums, J. D., Smith, C. W. & Simon, S. I. (1996) Biophys J 71, 3488-3500.

114. Berg, E. L., Magnani, J., Warnock, R. A., Robinson, M. K. & Butcher, E. C. (1992) Biochem Biophy Res Commun 184, 1048-1055.

115. Berg, E. L., Robinson, M. K., Mansson, O., Butcher, E. C. & Magnani, J. L. (1991) J Biol Chem 266, 14869-14872.

116. Pouyani, T. & Seed, B. (1995) Cell 83, 333-343.

117. Sako, D., Comess, K. M., Barone, K. M., Camphausen, R. T., Cumming, D. A. & Shaw, G. D. (1995) Cell 83, 323-331.

118. Wilkins, P. P., McEver, R. P. & Cummings, R. D. (1996) J Biol Chem 270, 22677-22680.

119. Alon, R., Feizi, T., Yuen, C. T., Fuhlbrigge, R. C. & Springer, T. A. (1995) J Immunol 154, 5356-5366.

120. Labow, M. A., Norton, C. R., Rumberger, J. M., Lombard-Gillooly, K. M., Shuster, D. J., Hubbard, J., Bertko, R., Knaack, P. A., Terry, R. W., Harbison, M. L., Kontgen, F., Stewart, C. L., McIntyre, K. W., Will, P. C., Burns, D. K. & Wolitzky, B. A. (1994) Immunity 1, 709-720.

121. Moore, K. L., Stults, N. L., Diaz, S., Smith, D. F., Cummings, R. D., Varki, A. & McEver, R. P. (1992) J Cell Biol 118, 445-456.

122. Norman, K. E., Moore, K. L., McEver, R. P. & Ley, K. (1995) Blood 86, 4417-4421.

123. Borges, E., Pendl, G., Eytner, R., Moll, T., Steegmaier, M., Zollner, O. & Vestweber, D. (1997) Blood 90, 1934-1942.

124. Borges, E., Tietz, W., Steegmaier, M., Moll, T., Hallmann, R., Hamann, A. & Vestweber, D. (1997) J Exp Med 185, 573-578.

125. Laszik, Z., Jansen, P. J., Cummings, R. D., Tedder, T. F., McEver, R. P. & Moore, K. L. (1996) Blood 88, 3010-3021.

126. Ruoslahti, E. & Pierschbacher, M. D. (1987) Science 238, 491-497.

127. Willemsen, O. H., Snel, M. M. E., Werf, K. O. v. d., Grooth, B. G. d., Greve, J., Hinterdorfer, P., Gruber, H. J., Schindler, H., Kooyk, Y. v. & Figdor, C. G. (1998) Biophys J 75, 2220-2228.

128. Fujisawa, N., Poole-Warren, L. A., Woodard, J. C., Bertram, C. D. & Schindhelm, K. (1999) Biomaterials 20, 955-962.

129. Dubreiul, R. R. (1991) BioEssays 13, 219-226.

130. Schakenraad, J. M., Busscher, H. J., Wildevuur, C. R. & Arends, J. (1986) J Biomed Mater Res 20, 773-84.

131. Bentley, K. L. & Klebe, R. J. (1985) J Biomed Mater Res 19, 757-769.

132. Curtis, A. & WIlkinson, C. (1997) Biomaterials 18, 1579-1583.

133. Schmidt, J. A. & Recum, A. F. v. (1992) Biomaterials 13, 1059-1069.

134. den Braber, E. T. d., Ruijter, J. E. d., Ginsel, L. A., Recum, A. F. v. & Jansen, J. A. (1998) J Biomed Mater Res 40, 291.

135. Britland, S., Morgan, H., Wojiak-Stondart, B., Riehle, M., Curtis, A. & Wilkinson, C. (1996) Exp Cell Res 228, 313-325.

136. den Braber, E. T., de Ruijter, J. E., Smits, H. T. J., Ginsel, L. A., von Recum, A. F. & Jansen, J. A. (1995) J Biomed Mater Res 29, 511-518.

137. Britland, S., Clark, P., Connolly, P. & Moores, G. (1992) Exp Cell Res 198, 124-129.

138. Xiao, Y. & Truskey, G. A. (1996) Biophys. J. 71, 2869-2884.

139. Walboomers, X. F., Croes, H. J. E., Ginsel, L. A. & Jansen, J. A. (1998) Biomaterials 19, 1861-1868.

140. Potember, R. S., Matsuzawa, M. & Liesi, P. (1995) Synthetic Metals 71, 1997-1999.

141. Healy, K. E., Thomas, C. H., Rezania, A., Kim, J. E., McKeown, P. J., Lom, B. & Hockberger, P. E. (1996) Biomaterials 17, 195-208.

142. Rezania, A., Thomas, C. H. & Healy, K. E. (1997) Ann Biomed Eng 25, 190-203.

143. den Braber, E. T. d., Ruijter, J. E. d. & Jansen, J. A. (1997) J Biomed Mater Res 37, 539-547.

144. Recum, A. F. v. & Kooten, T. G. v. (1995) J Biomater Sci Polymer Edn 7, 181-198.

145. Walboomers, X. F., Croes, H. J. E., Ginsel, L. A. & Jansen, J. A. (1999) J Biomed Mater Res 47, 204-212.

146. Walboomers, X. F., Monaghan, W., Curtis, A. S. G. & Jansen, J. A. (1999) J Biomed Mater Res 46, 212-220.

147. Walboomers, X. F., Croes, H. J. E., Ginsel, L. A. & Jansen, J. A. (1998) J Biomed Mater Res 42, 634-641.

148. Walboomers, X. F. & Jansen, J. A. (2000) Biomaterials 21, 629-636.

BIOGRAPHICAL SKETCH

In 1979, the author was born in Tianjin, a small industrial city of 10 million people, in the People's Republic of China. His father and grandfather, both engineers, named him "engineering achiever." They hoped, that as the first male child of both his father's and mother's families, the author would be successful. For seven years, he lived an insouciant life as the spoiled scion of two well-to-do families. In 1987, the author and his mother immigrated to Gainesville, Florida, to join his father, who was a Ph.D. candidate in Engineering Mechanics at the University of Florida.

Like a fly in amber, he was trapped in Gainesville by fate and circumstance for the next 13 years. After graduating from the international baccalaureate program at Eastside high school, the author enrolled at the University of Florida in the summer of 1996, and majored in Materials Science and Engineering. In May of 1996, he began an illustrious relationship with Dr. Anthony Brennan. Initially, the author worked on sol-gel organic-inorganic hybrid composites with Tom Miller, then a Ph.D. candidate. Then, in 1998, the author switched to working with the atomic force microscope, which is an integral part of his thesis. In the summer of 1998, the author worked for Exxon Chemical, under the supervision of Dr. Michael Zamora, a former student of Dr. Brennan.

After his experience at Exxon, the author decided to switch to biomedical engineering, and started a combined BS/MS program. To finish the program in 4 years,

the author took a prodigious number of classes, including 10 in the fall of 1998. As part of the biomedical engineering program, he engaged in clinical shadowing in the spring of 1999. While shadowing Dr. Keith Ozaki, a vascular surgeon, who graciously contributed to the author's thesis, the author realized that he wanted to be a surgeon. So the author took the MCAT, and applied to medical school. During the summer of 1999, with the reluctant permission of Dr. Brennan, the author traveled and studied in Europe. Upon his return, the author worked on his thesis while also interviewing for medical school. On June 20th, 2000, the author will begin a two-year stint as a secondary school science teacher in Ghana for the Peace Corps. Then in 2002, the author will matriculate at Northwestern University Medical School.